

# Small Language Models Offer Significant Potential for Science Community

Jian Zhang (张健)<sup>1\*</sup>

<sup>1</sup> School of Geophysics and Geomatics, China University of Geosciences, Wuhan 430074, China

\*Correspondence to: Jian Zhang, zhangjian@cug.edu.cn

**Abstract** Recent advancements in natural language processing, particularly with large language models (LLMs), are transforming how scientists engage with the literature. While the adoption of LLMs is increasing, concerns remain regarding potential information biases and computational costs. Rather than LLMs, I developed a framework to evaluate the feasibility of precise, rapid, and cost-effective information retrieval from extensive geoscience literature using freely available small language models (MiniLMs). A curated corpus of approximately 77 million high-quality sentences, extracted from 95 leading peer-reviewed geoscience journals such as *Geophysical Research Letters* and *Earth and Planetary Science Letters* published during years 2000 to 2024, was constructed. MiniLMs enable a computationally efficient approach for extracting relevant domain-specific information from these corpora through semantic search techniques and sentence-level indexing. This approach, unlike LLMs such as ChatGPT-4 that often produces generalized responses, excels at identifying substantial amounts of expert-verified information with established, multi-disciplinary sources, especially for information with quantitative findings. Furthermore, by analyzing emotional tone via sentiment analysis and topical clusters through unsupervised clustering within sentences, MiniLM provides a powerful tool for tracking the evolution of conclusions, research priorities, advancements, and emerging questions within geoscience communities. Overall, MiniLM holds significant potential within the geoscience community for applications such as fact and image retrievals, trend analyses, contradiction analyses, and educational purposes.

## Key points:

- A framework integrating small language models with an extensive and high-quality corpus of sentences from geoscience journals was established
- This framework facilitates precise and cost-effective knowledge transfer within geosciences, improving the reliability of information extraction
- Analyzing emotional tone and topical clusters within sentences aids in understanding perspectives on critical issues such as climate change

**Plain Language Summary** The field of geoscience (or any other field) has experienced an unprecedented burst in research publications, reflecting a rapidly advancing understanding of our planet. This expansion has resulted in an increasingly complex body of knowledge and a cognitive overload, while a concurrent shift towards interdisciplinary and transdisciplinary research poses challenges to effective and cheap knowledge transfer. To address these challenges, this perspective introduces an approach that leverages the extensive body of Earth science literature. By analyzing millions of individual sentences extracted from literature using small language models, the method enables a cost-effective and precise means of acquiring professional knowledge. Integrating semantic analysis with large language model summarization, the method has the potential to yield more specialized and quantitative insights than current excellent models like ChatGPT-4.

## 1 Introduction

The field of Earth science is undergoing rapid evolution in the Anthropocene, largely driven by the integration of artificial intelligence (AI) technologies. This necessitates robust interdisciplinary collaborations between computer science, data science, and geoscience (Bergen *et al.*, 2019; Cui, 2021; Li *et al.*, 2023). Such collaborations are increasingly vital given the pervasive impacts of climate change (Nielsen & D'haen, 2014). The Earth is a complex, interconnected, and dynamic system (Vance *et al.*, 2024), characterized by intricate human-environment relationships, complicated physical, dynamic, and chemical interactions, and variations across multiple temporal and spatial scales. For instance, river basins emerge from the complex interplay among land, biosphere, atmosphere, and human systems, exhibiting significant uncertainties across both temporal and spatial scales (Best, 2019). Precipitation, a vital component of the water cycle, links the hydrosphere, lithosphere, biosphere, and atmosphere (Wu *et al.*, 2020). These inherent complexities present substantial challenges for researchers seeking to acquire comprehensive and nuanced understanding.

Recent advancements in natural language processing, particularly in large language model (LLM) technology, offer substantial new avenues for scientific research. These models possess the potential to transform scientific practices. For example, LLMs can significantly enhance the efficiency and scale of ecological research (Gougherty & Clipp, 2024). Furthermore, LLMs such as the Generative Pre-trained Transformer (GPT) can be readily adapted for various tasks in chemistry and materials science by fine-tuning them to provide accurate responses to scientific queries expressed in natural language (Jablonka *et al.*, 2024).

However, it is crucial to acknowledge that responses generated by LLMs can sometimes be misleading, inaccurate, or factually incorrect (Foroumandi *et al.*, 2023). Therefore, validating information derived from LLMs against established sources, such as peer-reviewed publications and scholarly books, is essential (Foroumandi *et al.*, 2023). Furthermore, the black-box nature of LLMs often obscures the reasoning behind their predictions (Ott *et al.*, 2023). Additionally, the current limitations in accessing external knowledge sources can restrict the utility of LLMs in scientific applications (M. Bran *et al.*, 2024). As Li *et al.* (2023) noted, “While foundation models have had great success in applications such as natural language processing, how or if they could be applied in geosciences remains to be seen.”

Peer-reviewed publications constitute the primary repository of high-quality scientific knowledge, often containing latent insights relevant to future discoveries (Tshitoyan *et al.*, 2019). However, the unstructured nature and substantial heterogeneity within these publications present a significant obstacle to large-scale information analysis (Kononova *et al.*, 2021).

Corpus is the heart of a language model. Authoritative and curated sources is crucial for the creation of LLM applications for science (Ramachandran & Bugbee, 2025). Leading journals, such as *Geophysical Research Letters*, *Earth and Planetary Science Letters*, and *Nature Geoscience*, represent primary sources for constructing high-quality corpora in the geosciences. These publications encapsulate the collective expertise and insights of numerous researchers, reflecting a substantial accumulation of knowledge spanning decades. By developing a comprehensive corpus from these authoritative sources and leveraging high-performance language models, research capabilities could be significantly augmented, potentially facilitating the generation of novel hypotheses. It is noteworthy that a language model does not necessarily need to be large; large models may sometimes limit their applicability and interpretability.

## 2 Material and Method

### 2.1 Journal sources

The data is derived from a broad range of geoscience journals published by major academic entities. These include the Nature portfolio, Elsevier, Wiley, Springer, the American Association for the Advancement of Science (AAAS), the American Meteorological Society (AMS), the American Geophysical Union (AGU), and the European Geosciences Union (EGU). Collectively, these sources provide a robust and rigorous body of peer-reviewed geoscience research.

### 2.2 Standardized literature

From these journal sources, approximately 95 highly reputable geoscience journals were rigorously selected in this perspective. This selection includes prominent publications such as *Nature Geoscience*, *Geophysical Research Letters*, *Journal of Geophysical Research*, *Remote Sensing of Environment*, *Earth-Science Reviews*, *Science Advances*, *Earth and Planetary Science Letters*, *Journal of the Atmospheric Sciences*, *Geochimica et Cosmochimica Acta*, *Environmental Science & Technology*, *Geology*, *Proceedings of the National Academy of Sciences*, and *Water Research*. These journals represent a broad spectrum of geoscience disciplines, including atmospheric science, space science, hydrology, environmental science, remote sensing, oceanography, ecology, and geophysics.

Consequently, I compiled a dataset of over 376,000 articles published between 2000 and 2024. To ensure consistency, Portable Document Format (PDF) filenames adhere to a standardized format: “journal abbreviation–year of publication–title.” A comprehensive list of journal names, their corresponding abbreviations, and the total article count for each journal is available in Table 1.

**Table 1.** *Journal and sentence information. This table delineates comprehensive information about the journal, encompassing its full name, International Organization for Standardization (ISO) abbreviation (only the Latin letters are retained), years of literature coverage, total number of published articles, and the aggregate literature sentences.*

Full name of journal	ISO Abbreviation	Years	Article no.	Sentence no.
<i>Geophysical Research Letters</i>	<i>GeophysResLett</i>	2002–2024	31,820	3,305,108
<i>Earth's Future</i>	<i>EarthsFuture</i>	2014–2024	1,479	344,903
<i>Reviews of Geophysics</i>	<i>RevGeophys</i>	2002–2024	443	174,007
<i>Water Resources Research</i>	<i>WaterResourRes</i>	2002–2024	11,669	2,597,772
<i>Journal of Geophysical Research: Atmospheres</i>	<i>JGeophysResAtmos</i>	2002–2024	17,458	3,953,872
<i>Journal of Geophysical Research: Oceans</i>	<i>JGeophysResOceans</i>	2002–2024	9,206	2,089,057
<i>Journal of Geophysical Research: Planets</i>	<i>JGeophysResPlanets</i>	2002–2024	3,770	890,708
<i>Journal of Geophysical Research: Space Physics</i>	<i>JGeophysResSpacePhys</i>	2002–2024	13,907	2,741,795
<i>Journal of Geophysical Research: Solid Earth</i>	<i>JGeophysResSolidEarth</i>	2002–2024	10,628	2,471,150
<i>Journal of Geophysical Research: Biogeosciences</i>	<i>JGeophysResBiogeosci</i>	2005–2024	3,524	749,651
<i>Journal of Geophysical Research: Earth Surface</i>	<i>JGeophysResEarthSurf</i>	2003–2024	2,778	693,676
<i>Space Weather</i>	<i>SpaceWeather</i>	2003–2024	1,549	296,054
<i>AGU Advances</i>	<i>AGUAdv</i>	2020–2024	200	47,092
<i>Journal of Geophysical Research: Machine Learning and Computation</i>	<i>JGeophysResMachLearnCom put</i>	2024–2024	62	17,741
<i>Journal of Advances in Modeling Earth Systems</i>	<i>JAdvModelEarthSyst</i>	2009–2024	2,017	508,536
<i>Perspectives of Earth and Space Scientists</i>	<i>PerspectEarthSpaceSci</i>	2023–2024	16	2,947
<i>Geochemistry Geophysics Geosystems</i>	<i>GeochemGeophysGeosyst</i>	2002–2024	5,300	1,069,332
<i>Radio Science</i>	<i>RadioSci</i>	2023–2024	69	12,616
<i>Global Biogeochemical Cycles</i>	<i>GlobBiogeochemCycle</i>	2002–2024	2,530	535,221

<i>Earth and Space Science</i>	<i>EarthSpaceSci</i>	2014–2024	1,610	332,285
<i>Tectonics</i>	<i>Tectonics</i>	2023–2024	118	34,688
<i>Global Environmental Change-human And Policy Dimensions</i>	<i>GlobEnvirnChangeHumanPolicyDimens</i>	2010–2024	1,895	476,964
<i>Earth and Planetary Science Letters</i>	<i>EarthPlanetSciLett</i>	2004–2024	10,001	1,867,375
<i>Earth-Science Reviews</i>	<i>EarthSciRev</i>	2009–2024	2,706	1,020,985
<i>ISPRS Journal of Photogrammetry and Remote Sensing</i>	<i>ISPRSJPhotogrammRemoteSens</i>	2000–2024	3,067	812,215
<i>Journal of Hydrology</i>	<i>JHydrol</i>	2009–2024	14,280	3,360,058
<i>Remote Sensing of Environment</i>	<i>RemoteSensEnviron</i>	2003–2024	7,596	1,924,737
<i>Water Research</i>	<i>WaterRes</i>	2003–2024	15,161	2,904,672
<i>Weather and Climate Extremes</i>	<i>WeatherClimExtremes</i>	2013–2024	634	138,841
<i>Agricultural and Forest Meteorology</i>	<i>AgricForMeteorol</i>	2009–2024	4,208	921,866
<i>Geochimica et Cosmochimica Acta</i>	<i>GeochimCosmochimActa</i>	2009–2024	6,832	1,783,798
<i>Advances in Water Resources</i>	<i>AdvWaterResour</i>	2009–2024	2,781	702,577
<i>One Earth</i>	<i>OneEarth</i>	2019–2024	435	50,131
<i>Science Bulletin</i>	<i>SciBull</i>	2016–2024	3,098	371,702
<i>Lancet Planetary Health</i>	<i>LancetPlanetHealth</i>	2017–2024	387	51,932
<i>Renewable and Sustainable Energy Reviews</i>	<i>RenewSustEnergRev</i>	2009–2024	12,850	3,548,197
<i>Environment International</i>	<i>EnvironInt</i>	2009–2024	6,576	1,307,122
<i>Applied Geography</i>	<i>ApplGeogr</i>	2009–2024	2,202	482,631
<i>Cities</i>	<i>Cities</i>	2010–2024	3,068	772,181
<i>Computers, Environment and Urban Systems</i>	<i>ComputEnvironUrbanSyst</i>	2009–2021	817	205,200
<i>Journal of Hazardous Materials</i>	<i>JHazardMater</i>	2009–2024	14,592	2,690,139
<i>Geoderma</i>	<i>Geoderma</i>	2009–2024	4,847	979,260
<i>International Journal of Applied Earth Observation and Geoinformation</i>	<i>IntJApplEarthObsGeoinf</i>	2009–2024	2,773	599,791
<i>Journal of Rural Studies</i>	<i>JRuralStud</i>	2010–2024	1,995	565,611
<i>Landscape and Urban Planning</i>	<i>LandscUrbanPlan</i>	2009–2024	2,326	495,518
<i>Land Use Policy</i>	<i>LandUsePol</i>	2009–2024	4,980	1,231,936
<i>Nature Geoscience</i>	<i>NatGeosci</i>	2007–2024	2,014	182,328
<i>Communications Earth &amp; Environment</i>	<i>CommunEarthEnviron</i>	2020–2024	1,085	170,353
<i>Nature Ecology &amp; Evolution</i>	<i>NatEcolEvol</i>	2016–2024	736	80,675
<i>Nature Reviews Earth &amp; Environment</i>	<i>NatRevEarthEnviron</i>	2019–2024	91	20,412
<i>Nature Climate Change</i>	<i>NatClimChang</i>	2011–2024	1,158	108,836
<i>Nature Water</i>	<i>NatWater</i>	2023–2024	41	8,395
<i>Nature Communications (Geoscience only)</i>	<i>NatCommun</i>	2014–2024	4,961	651,741
<i>npj Climate and Atmospheric Science</i>	<i>npjClimAtmosSci</i>	2018–2024	519	78,739
<i>Nature (Geoscience only)</i>	<i>Nature</i>	2009–2024	1,449	164,475
<i>Nature Sustainability</i>	<i>NatSustain</i>	2018–2024	434	56,801
<i>Nature Energy</i>	<i>NatEnergy</i>	2015–2024	406	55,454
<i>Atmospheric Chemistry and Physics</i>	<i>AtmosChemPhys</i>	2001–2024	12,461	3,298,928
<i>Earth System Science Data</i>	<i>EarthSystSciData</i>	2009–2024	1,200	269,809
<i>Atmospheric Measurement Techniques</i>	<i>AtmosMeasTech</i>	2008–2024	4,367	1,124,558
<i>Hydrology and Earth System Sciences</i>	<i>HydrolEarthSystSci</i>	2001–2024	4,872	1,222,152
<i>Journal of Applied Meteorology and Climatology</i>	<i>JApplMeteorolClimatol</i>	2010–2024	2,072	473,546
<i>Journal of the Atmospheric Sciences</i>	<i>JAtmosSci</i>	2003–2024	4,196	1,070,337
<i>Journal of Climate</i>	<i>JClim</i>	2000–2024	9,364	2,146,492
<i>Monthly Weather Review</i>	<i>MonWeatherRev</i>	2005–2024	4,343	1,083,666
<i>Journal of Atmospheric and Oceanic Technology</i>	<i>JAtmosOceanTechnol</i>	2005–2024	2,806	612,599
<i>National Science Review (Geoscience only)</i>	<i>NatlSciRev</i>	2014–2020	105	11,799
<i>Geology</i>	<i>Geology</i>	2003–2020	3,756	81,821
<i>Science (Geoscience only)</i>	<i>Science</i>	2014–2024	415	21,153
<i>Science Advances (Geoscience only)</i>	<i>SciAdv</i>	2015–2024	2,147	398,591
<i>Environmental Science &amp; Technology</i>	<i>EnvironSciTechnol</i>	2010–2024	21,060	3,024,293
<i>Environmental Research Letters</i>	<i>EnvironResLett</i>	2010–2020	2,264	343,357
<i>Global Change Biology</i>	<i>GlobChangeBiol</i>	2013–2024	3,209	440,763
<i>Ecology Letters</i>	<i>EcolLett</i>	2013–2024	1,973	352,645
<i>Ecological Monographs</i>	<i>EcolMonogr</i>	2010–2024	492	157,715
<i>Land Degradation &amp; Development</i>	<i>LandDegradDev</i>	2010–2024	3,061	570,632
<i>Global Ecology and Biogeography</i>	<i>GlobEcolBiogeogr</i>	2013–2024	151	26,350
<i>Wiley Interdisciplinary Reviews-Climate Change</i>	<i>WileyInterdiscipRevClimChan</i>	2013–2024	330	73,138
<i>Wiley Interdisciplinary Reviews-Water</i>	<i>WileyInterdiscipRevWater</i>	2018–2024	338	77,307

<i>IEEE Geoscience and Remote Sensing Magazine</i>	<i>IEEEGeosciRemoteSensMag</i>	2015–2024	288	58,936
<i>IEEE Journal of Selected Topics in Applied Earth Observations and Remote Sensing</i>	<i>IEEEJSelTopApplEarthObser vRemoteSens</i>	2015–2024	3,400	747,643
<i>IEEE Transactions on Geoscience and Remote Sensing</i>	<i>IEEETransGeosciRemoteSens ing</i>	2001–2024	12,489	2,950,842
<i>Science China- Earth Sciences</i>	<i>SciChinaEarthSci</i>	2016–2024	1,073	215,832
<i>Current Climate Change Reports</i>	<i>CurrClimChangRep</i>	2015–2024	131	24,846
<i>Climatic Change</i>	<i>ClimChange</i>	2010–2024	2,871	478,813
<i>Mathematical Geosciences</i>	<i>MathGeosci</i>	2010–2024	588	108,302
<i>Journal of Geodesy</i>	<i>JGeodesy</i>	2010–2024	938	209,072
<i>International Journal of Geographical Information Science</i>	<i>IntJGeogrInfSci</i>	2010–2023	1,357	316,206
<i>Urban Geography</i>	<i>UrbanGeogr</i>	2009–2023	953	207,811
<i>Annals of the American Association of Geographers</i>	<i>AnnAmAssocGeogr</i>	2009–2024	1,158	236,741
<i>Critical Reviews in Environmental Science and Technology</i>	<i>CritRevEnvironSciTechnol</i>	2010–2021	566	183,037
<i>Annual Review of Environment and Resources</i>	<i>AnnuRevEnvironResour</i>	2005–2024	279	89,135
<i>Annual Review of Marine Science</i>	<i>AnnuRevMarSci</i>	2012–2024	240	64,239
<i>Annual Review of Earth and Planetary Sciences</i>	<i>AnnuRevEarthPlanetSci</i>	2007–2024	478	152,760
<i>Proceedings of the National Academy of Sciences of the United States of America (Geoscience only)</i>	<i>ProcNatAcadSciUSA</i>	2007–2024	2,036	225,256

### 2.3 Body text identification and sentence splitting

Due to the intricate formatting of PDF documents, which incorporates elements like icons, publisher and article details, figures, tables, and their associated captions, accurate extraction of body text is challenging. I addressed this issue by focusing on the extraction of the “Abstract” and main body text, while deliberately excluding sections such as the “Reference”. For articles with two- or three-column layouts, text segmentation was implemented on each page to mimic human reading habit. Sentence segmentation relied on the period character (“.”), with exceptions made for common abbreviations such as “et al.”, “Fig.”, and “Tab.”. Sentences longer than 256 or shorter than 10 words were discarded. The final processed dataset comprised 76,862,981 extracted sentences (Tab. 1).

**Table 2.** List of pre-trained sentence transformer models. This table delineates the comprehensive nomenclature, abbreviated designation, maximum sequence length, vector dimensionality, and overall model size of the respective models, where “M” denotes million and “B” signifies billion.

Full name of Model	abbr.	Max Sequence Length	Dimension	Model Size
<i>all-MiniLM-L6-v2</i>	<i>PSTM_1</i>	256	384	22.7 M
<i>all-MiniLM-L12-v2</i>	<i>PSTM_2</i>	256	384	33.4 M
<i>all-mpnet-base-v2</i>	<i>PSTM_3</i>	384	768	109 M
<i>mxbai-embed-large-v1</i>	<i>PSTM_4</i>	512	1,024	335 M
<i>multilingual-e5-large-instruct</i>	<i>PSTM_5</i>	512	1,024	560 M
<i>SFR-Embedding-Mistra</i>	<i>PSTM_6</i>	4,096	4,096	7.11 B

### 2.4 Topic selection and word embedding

To minimize computational requirements, a keyword-based approach was initially employed to identify and match sentences across the entire corpus. For instance, in studies focused on precipitation, keywords such as “precipitation” (case-insensitive) and “rain” (case-insensitive) were utilized. These filtered sentences were then encoded into dense vectors using six pre-trained sentence transformer models (PSTMs), which have demonstrated high performance in the Massive Text Embedding Benchmark (MTEB). The selected PSTMs encompass both lightweight models, including *all-MiniLM-L6-v2* and *all-MiniLM-L12-v2* (Reimers & Gurevych, 2019a), designed

for a balance of speed and performance, and medium-to-large models like *SFR-Embedding-Mistral* (Meng *et al.*, 2024). The parameter counts of these models range significantly, from 22.7 million to 7.11 billion, with dense vector embeddings having dimensionalities ranging from 384 to 4096. The maximum input token sequence length varies from 256 to 4096 tokens (detailed parameters are available in Table 2). It should be noted that top-performing models on the MTEB benchmark do not necessarily transfer effectively to specific tasks (Reimers & Gurevych, 2019b).

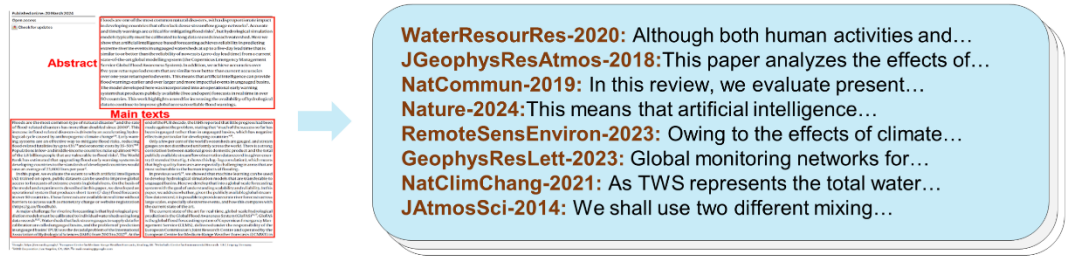
## Journal sources



## Standardized literatures



## Main texts identification & sentence splitting



## Topic selection & word embedding



## Downstream tasks

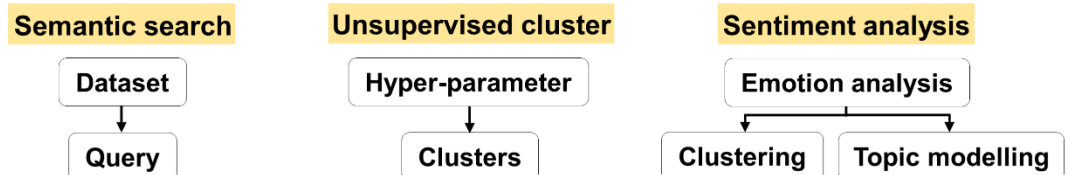


**Figure 1.** The concept diagram of sentence-level MiniLM approaches for geosciences. The methodology follows a hierarchical framework: initially, literature sources are compiled and standardized (refer to Tab. 1 for journal abbreviations). Subsequently, body texts are identified and segmented into individual sentences (see Tabs. 1 total sentence counts). Following this, topics are selected, and word embeddings are generated (see Tab. 2 for details on PSTMs). Finally, three downstream tasks are executed: Task 1 (semantic search) is illustrated in Figs. 2–3 and Figs. S1–S11; Task 2 (clustering) is represented in Figs. 4–5; and Task 3 (sentiment analysis) is shown in Figs. 6–7 and Tabs. S1–S2.

## 2.5 Downstream tasks

### 2.5.1 Sentence-level semantic search

For this task, PSTMs were utilized to encode both the text corpora and the user-submitted query into dense vector representations. Similarity scores between the corpora and query were calculated by taking the inner product

of their respective vectors, where higher scores signify greater relevance. For the ensemble model, a final relevance ranking was produced by averaging the similarity scores derived from the six individual PSTMs. The highest-ranked sentences were then processed by LLMs (Llama, DeepSeek or ChatGPT-4) to automatically summarize the main themes.

### 2.5.2 Sentence-level unsupervised clustering

To prepare for unsupervised clustering using dense vectors obtained from a PSTM, the categorization of sentences into meaningful groups is practicable. For instance, sentences can be grouped by their year of publication. Agglomerative Clustering was selected as the clustering method because it allows for the specification of a merging threshold. This is beneficial when the actual number of clusters is unclear, allowing for the manual control of cluster granularity through modification of the threshold. In addition, hyperparameters such as a minimum cluster count and a minimum similarity score are necessarily defined.

### 2.5.3 Sentence-level sentiment analysis

The *go-emotion* language model architecture can categorize sentences into 27 separate emotion classes, such as “admiration,” “confusion,” “approval,” and “disappointment” (Demszky *et al.*, 2020). The *Twitter-RoBERTa-base-sentiment-latest* language model can classify sentences as exhibiting negative, positive, or neutral sentiment. Sentences identified as expressing specific sentiments can be further analyzed using topic modeling (e.g., with the *BERTopic* language model) or unsupervised clustering. Figure 1 illustrates the full method workflow.

## 3 Downstream tasks

### 3.1 Sentence-level semantic search

Gaining in-depth knowledge within any field demands substantial effort. For instance, although the general impact of climate change on precipitation patterns is widely acknowledged, the nuanced details are often unavailable to those without specialized training in climatology. To investigate this relationship, all relevant sentences were first filtered. Then, PSTMs were employed to perform a semantic search and identify the most pertinent historical sources using the query: “The pattern of precipitation is modified by climate change” (Figure 2). While more complex models generally yielded higher similarity scores than a lightweight model like PSTM\_1, a significant score variance of approximately 0.1 across the six models was found. This suggests that even advanced models may fail to identify the most relevant sources when used in isolation. Therefore, an ensemble model, which arithmetically averages the similarity scores of all six PSTMs, probably provides a more reliable and robust ranking system. Applying the L2 norm to assess the difference between individual PSTM scores and the average score reveals that PSTM\_5 has the greatest influence on the average (29.8%), with PSTM\_6 having the smallest influence (7.2%). The top-ranked sentences identified by this ensemble model effectively illustrate the complex ways in which climate change influences precipitation (Fig. 2b). Finally, a comprehensive summary was created from the top ranked sentences (5,000 in this analysis) using a pre-trained LLM (Llama 2 70B), and this summary effectively elucidates the intricate roles of climate change in modifying precipitation patterns.

While effective, keyword-based sentence filtering is limited by its inability to consider semantic context and the surrounding context. To address these limitations, I further developed a search software that can utilize all the aforementioned corpus in Tab.1. Through simple question-based queries, the software can rapidly identify the most relevant sentences and their corresponding literature sources, as illustrated in Figure 3. For example, a query such

as “radiosonde has a time interval of s” submitted to the software returned recommendations based on the PSTM\_3 model, along with the surrounding contextual sentences. This search yielded accurate technical specifications, indicating typical sampling frequencies of 1 or 2 seconds for modern radiosondes, with standard release time at 0000 and 1200 UTC. In contrast, ChatGPT-4 provided inaccurate results for the same query. Further direct comparisons between the software and ChatGPT-4 are presented in Figures S1–S6 in the Supporting Information. These results highlight the advantage of the software over ChatGPT-4, particularly for retrieving quantitative scientific data (e.g., turbulence dissipation rate in the lower atmosphere), navigating controversial scientific conclusions (e.g., wind changes under global change), or accessing less commonly known information (e.g., the download address of meteor radar data). The information provided by the search software is precise, comprehensive, and directly verifiable through the linked source file.

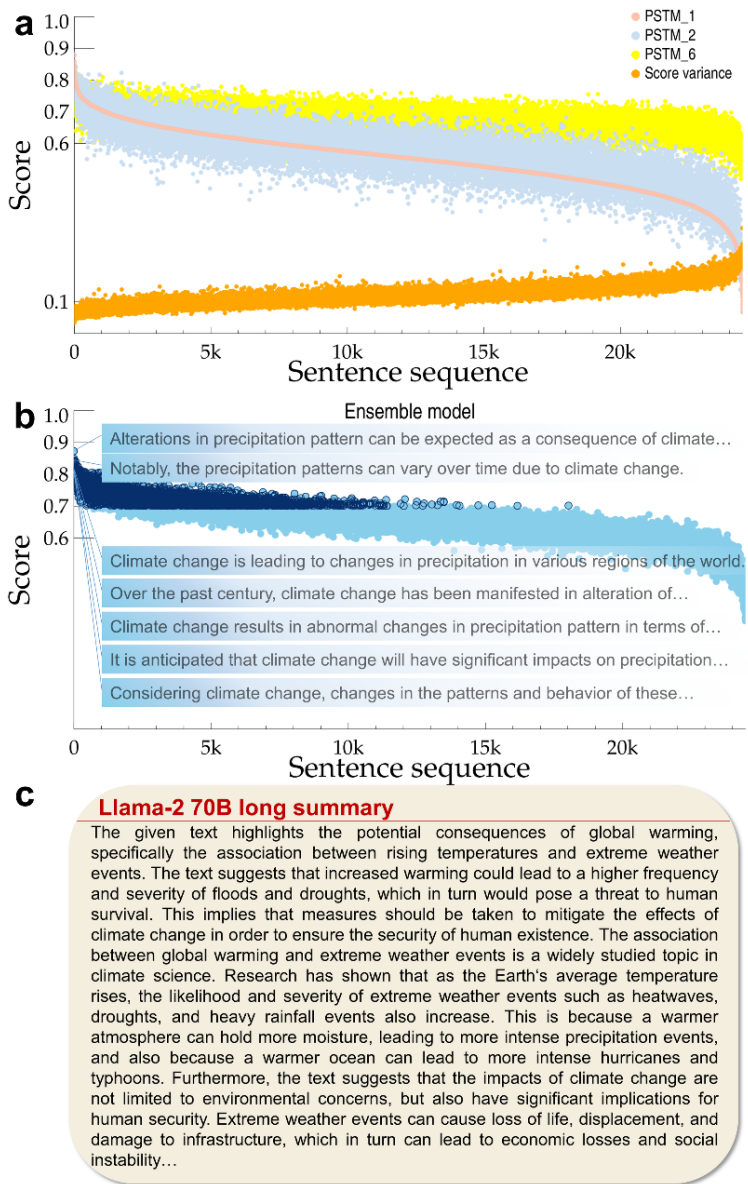


**Figure 2.** The query “The pattern of precipitation is modified by climate change” was utilized to demonstrate sentence-level semantic search. A corpus of 24,475 sentences containing “precipitation” (case-insensitive) or “rain” (case-insensitive) and “climate change” (case-insensitive) was used for analysis. Dot product similarity scores were calculated between the query and sentence embeddings. Sentences were sorted according to PSTM\_1 scores (light red), with corresponding PSTM\_2 (light blue) and PSTM\_6 (yellow) scores visualized in panel (a). The variance of scores across six models is indicated in orange. A comprehensive average score (panel b) was computed, and the top 5,000 ranked sentences are shown with dark blue outlines. The top 7 ranked sentences are shown in the figure. Panel (c) displays a part of summary generated using a pre-trained LLM (Llama 2 70B), prompted to “Please summarize provided text with at least 400 words”, based on the top 5,000 ranked sentences.

Moreover, the retrieval software can be effectively integrated with pre-trained LLMs. As demonstrated in Figures S7–S8, this hybrid approach, which combines semantic matching across the entire corpus with summarization of relevant sentences (similarity scores  $> 0.7$ ) and their surrounding context, yields comprehensive and nuanced summaries of complex topics, such as the influence of urban heat islands on precipitation and atmospheric gravity wave formation. However, the computational demands of this integrated approach currently limit its practical application when using ensemble models, as depicted in Figure 2.

radiosonde has a time interval of s
radiosonde has a time interval of s

0.76: For AIRS, we have collocated the measurements within  $\pm 3$  hr from 01:30 to 13:30 local time since the local equator crossing time of AIRS is close to these hours. **For radiosonde, we use the data at 00:00 UTC and within  $\pm 30$  min.** Also, we have collocated the satellite data within  $\pm 10$  km from the location of radiosonde. [IGRA-2023 Validation of INSAT-3D and INSAT-3DR Temperature Profile Retrievals Using Ground-Based Satellite and Radiosonde Data](#) [OPEN](#)

0.76: During 14–20 March and 4–9 August, strong echo layers continuously exist AA  $AA = 2.0\text{--}6.0$  km, although those present in August are not as clear as those at seen in March. **Radiosonde Observations During the campaigns, radiosonde observations were performed at 4-hr intervals (i.e., 03:30, 07:30, 11:30, 15:30, 19:30, and 23:30 UTC).** At 23:30 and 11:30 UTC, observations were made using RS-11G (Meisei electric), while the others were conducted using RS41-SGP (Vaisala Inc.) or RS-11G. The radiosondes measured temperature, horizontal winds, and humidity at 1-s intervals. [IGRA-2023-KelvinHelmholtz Billows in the Troposphere and Lower Stratosphere Detected by the FANSY Radar at Syowa Station in the Antarctic](#) [OPEN](#)

0.75: Instruments started sampling data from the surface at the locations specified in Figure 2 and then drifted by the mean flow and instrument velocity ( $ws$ ;  $m\ s^{-1}$ ) due to buoyancy. **The trajectory of the radiosonde,  $S$ , was calculated as the following:  $S \sqrt{Xt^2} + \int_0^t ws\ dt$  where  $Dt$  is the time interval of data sampling between two levels and was assigned to be 20 s.** The vertical velocity of the instrument,  $ws$ , was assumed to be  $5\ m\ s^{-1}$ . [IGRA-2011-Observing System Simulation Experiment Development of the system and preliminary results](#) [OPEN](#)

0.74: It takes approximately an hour for the balloon to rise to this level, hence the radiosondes are released one hour before the synoptic times. **The radiosonde takes measurements at intervals of approximately 2 s; high resolution data files contain all such data.** The standard resolution data files contain measurements taken at particular levels of the atmosphere. [IGRA-2008-Combined use of MODIS AVHRR and radiosonde data for the estimation of spatiotemporal distribution of precipitable water](#) [OPEN](#)

0.74: Cloud liquid layers are  $0.3\text{--}0.8$  km deep, while the liquid plus ice thickness is typically twice that depth. **Results related to radiosonde measurements are provided in Fig 7 and are based on time periods within 15 min of the radiosonde launch under the assumption that the conditions measured by the radiosondes will not change appreciably over that short time period.** The distribution of cloud-top temperatures, which largely determine the initial ice crystal growth regime, ranges from  $(cid:1)18^{\circ}$  to  $(cid:1)14^{\circ}\text{C}$ . The cloud top is most often near, or slightly above, the base of the temperature inversion, but can vary by a few hundred meters in either direction due to cloud-scale variability. [IAS-2008-Vertical Motions in Arctic Mixed-Phase Stratiform Clouds](#) [OPEN](#)

0.73: Vertical profiles of atmospheric temperature and humidity were obtained from radiosondes (DFM-09, Graw) from the KITcube observation system (Kalthoff et al., 2013) during IOPs. **Radiosondes were launched at 2 to 3-hr intervals and depending on height, the 1-s raw data are averaged over 2 s (between ground and 3 km), 4 s (3 and 10 km), and 8 s ( $> 10$  km).** In this study, we used in particular data from two IOPs (24 April 2013 and 19 May 2013) characterized by mostly clear-sky conditions with only few clouds in the morning and afternoon and weak winds. [IGRA-2018-Quantifying the Impact of Subsidence and Surface Physical Processes on the Predictive Skill of Subseasonal Mesoscale Atmospheric Simulations](#) [OPEN](#)

0.71: In the study presented in this paper, AMDAR data are the same as those used within operational data assimilation system at Slovenian Environment Agency. **Radiosondes [21] Radiosonde measurements have traditionally been made every 6 or 12 hours at few tens of stations over Europe.** Although these measurements are sparse, they have traditionally been the main source of upper-air information for NWP, and they remain a crucial wind information. [IGRA-2012-Validation of Mode-5 Meteorological Routine Air Report aircraft observations](#) [OPEN](#)

0.71: The zonal and omega wind profiles are available at 2.5 ( $cid:1$ ) 2.5 degree spatial resolution that may lead to overlap in retrieving time series profiles over three study locations (Delhi, Kanpur and Varanasi, Figure 2) as the ariel distance between cities is approximately 3.44( $cid:1$ ) or 382 km (DelhiKanpur) and 2.66( $cid:1$ ) or 295 km (Kanpur-Varanasi). **Radiosonde data are available twice daily at coordinated universal time (UTC) 0 and 12z (Figures 5a – 5c).** We have computed various stability indices (Figures 6 – 6g), based on radiosonde data, such as Total Totals (TT) (a combination of the vertical totals and the cross totals), Convective Available Potential Energy (CAPE), Maximum Lifted Index (LI), CAP strength, Lifted Index at 500 hPa and 300 hPa, Severe Weather Threat Index (SWEAT), convective temperature, K Index, low level (0 – 1 km) and deep layer (0 – 6 km) shear, precipitable water and wind direction and speed (surface – SFC to 6 km). [IGRA-2007-Influence of a dust storm on carbon monoxide and water vapor over the IndoGangetic Plain](#) [OPEN](#)

0.71: Radiosondes are the primary means of obtaining the vertical distribution of temperature and water vapor at the tropical ARM sites. **Radiosondes are launched at nominally 12-hour intervals (0000 and 1200 UTC), which is a much coarser time resolution than the profiles provided by the MMCR and other active remote sensors.** Cloud properties vary more rapidly than the water vapor profile, but water vapor can change significantly over the 12 hours between radiosonde launches. [IGRA-2007-Cloud properties and associated radiative heating rates in the tropical western Pacific](#) [OPEN](#)

0.70: These profiles are given at the model levels (91 from 1 January 2013 to 25 June 2013 at 18 UT and 137 from 26 June 2013 onward), and all model level pressure values can be computed from the surface pressure. **Radiosonde data are used for selected spectra measured within 70 min from the daily radiosonde launch (12 UTC).** Otherwise, an interpolation between radiosonde data and ECMWF data is performed. [IGRA-2019-Automatic Ice Cloud Identification and Properties Using Downwelling Spectral Radiance From 100 to 1400 cm \$^{-1}\$](#)  [OPEN](#)

0.70: Those uncertainty sources must be characterized and corrected if possible. **Moreover, radiosondes typically are launched at intervals of 12 h, a temporal resolution that is often not sufficient for many meteorological applications [Turner et al., 2003].** The objective of this study is to evaluate W retrievals from the AERONET network observations under different climatic conditions. [IGRA-2014-Evaluation of AERONET precipitable water vapor versus radiometric GPS and radiosondes at ARM sites](#) [OPEN](#)

0.69: Data and Method This study utilizes high vertical resolution radiosonde data collected at 120 stations across China. **Radiosondes are launched twice daily (00 and 12 UTC) and measure pressure, temperature, and wind speed profiles at time intervals of  $1.2 \pm 0.1$  s, providing data at a vertical resolution of approximately 6–8 m.** The data set spans the period from January 2011 to December 2018 and covers China's mainland from longitude  $76^{\circ}\text{E}$  to  $129.5^{\circ}\text{E}$  and latitude  $16.9^{\circ}\text{N}$  to  $49.2^{\circ}\text{N}$ . It encompasses diverse surface topographic features, including [km], and maximum height (km) of tropical convective regions, mid-latitude plains, basins, and the Qinghai-Tibetations in China. [IGRA-2024-Comparative Analysis of Gravity Wave Characteristics in China and the United States Using High Vertical Resolution Radiosonde Observations](#) [OPEN](#)

You radiosonde has a time interval of s
Ø

 A radiosonde typically transmits data at intervals of 4 to 6 seconds.
Therefore, a radiosonde has a time interval of 4-6 seconds.

**Figure 3.** I developed a software to illustrate semantic search capabilities within atmospheric science literature. To minimize computational requirements, only atmospheric-relevant journals such as *Geophysical Research Letters* and *Journal of Geophysical Research: Atmospheres* were selected. The software was run on a laptop equipped with an Intel® Core™ i7-10750H CPU @ 2.60GHz, 64GB of memory, and an NVIDIA Quadro P620 GPU. The bottom panel replicates a query generated by ChatGPT-4: “radiosonde has a time interval of s.” The top-matched sentences, identified by the PSTM\_3 model, are highlighted in orange, with the corresponding relevance score indicated numerically. Contextual sentences preceding and following the matched segments are displayed in black, with blue annotations denoting the original reference. An “OPEN” button facilitates direct access to the original publication in PDF format.

9

Academic debates often feature a diverse array of opinions, encompassing both favorable and unfavorable perspectives on a specific subject. As an example, Figure S9 uses two contrasting queries to illustrate this point: “Machine learning and deep learning have advantages in hydrological modeling” and “Machine learning and deep learning have limitations in hydrological modeling.” While these queries are apparently opposing, they show a high semantic similarity score of 0.95 when assessed by PSTM\_1. This may highlight the reduced capacity of lightweight PSTMs, such as PSTM\_1, to distinguish subtle semantic differences. However, medium-to-large PSTMs demonstrate enhanced performance in this domain. By mapping sentence collections into a 1,024-dimensional vector space with PSTM\_4, the temporal evolution of both the advantages and limitations of machine learning in hydrological modeling becomes clear. Notably, discourse on both these themes has increased significantly since 2021, which reflects the accelerating adoption of AI techniques in hydrological modeling. Analyzing this year-over-year variation allows researchers to gain valuable insights into research focuses and emerging uncertainties across different fields.

Moreover, semantic search offers a valuable approach for academic image retrieval. Utilizing the association between images and their corresponding captions, user prompts can be matched against a large corpus of captions to identify relevant images. I have also compiled a substantial dataset of high-resolution images (about 2 million) extracted from papers listed in Tab.1. Illustrative examples of software applications for image retrieval are provided in Figures S10–S11. This approach holds potential benefits for students, educators, and researchers.

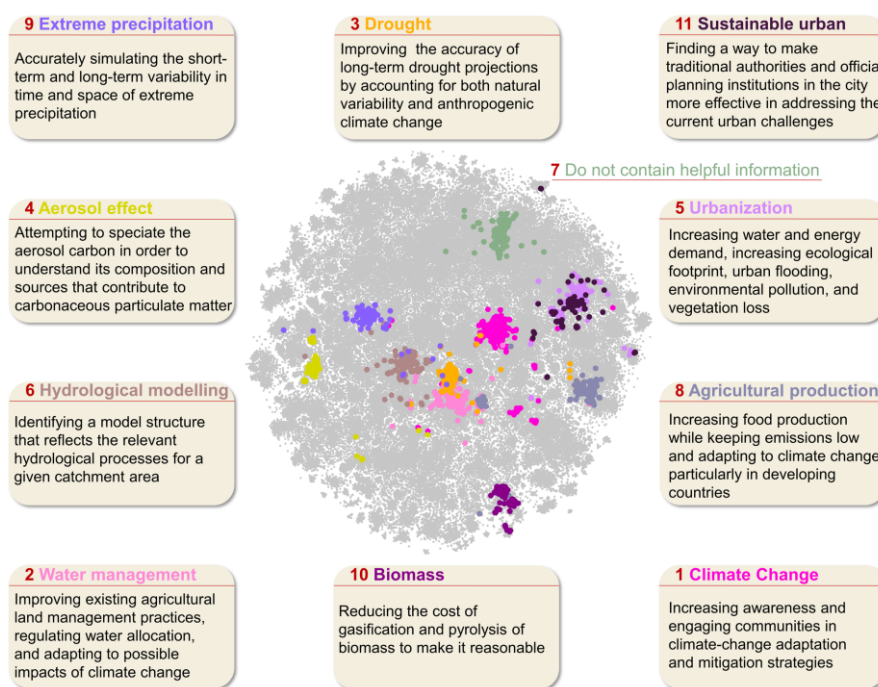


**Figure 4.** The application of sentence-level unsupervised clustering is illustrated through an analysis of texts containing the word “challenge” (case-insensitive). Unsupervised clustering was applied to 271,214 related records, resulting in the selection of the top 11 clusters (visualized as colored points in the figure). Sentences were embedded using PSTM\_1, and the minimum similarity score is 0.7 for clustering. A pre-trained LLM (Llama 2 7B) was then used to summarize each cluster’s content using the prompt, “Please summarize the challenge.” The 11 identified topics and their corresponding challenges are displayed around the scatter plot. Notably, cluster 7 predominantly contains short, declarative sentences with limited information.

### 3.2 Sentence-level unsupervised clustering

As depicted in Figure 4, I filtered a corpus comprising approximately 271,000 sentences to discern researcher perspectives regarding both historical and contemporary challenges. The ten most significant challenges identified by unsupervised clustering primarily revolve around concerns related to the risks of climate change and problems concerning water resources. As underscored by UN-Water (2021), the global community is not on track to achieve

critical Sustainable Development Goals (SDGs), especially SDG 6. Worryingly, nearly 80% of the global population is facing significant threats to water security, with one in three individuals lacking access to safe drinking water (Vörösmarty *et al.*, 2010). These issues are further intensified by the consequences of climate change (Ren *et al.*, 2024).

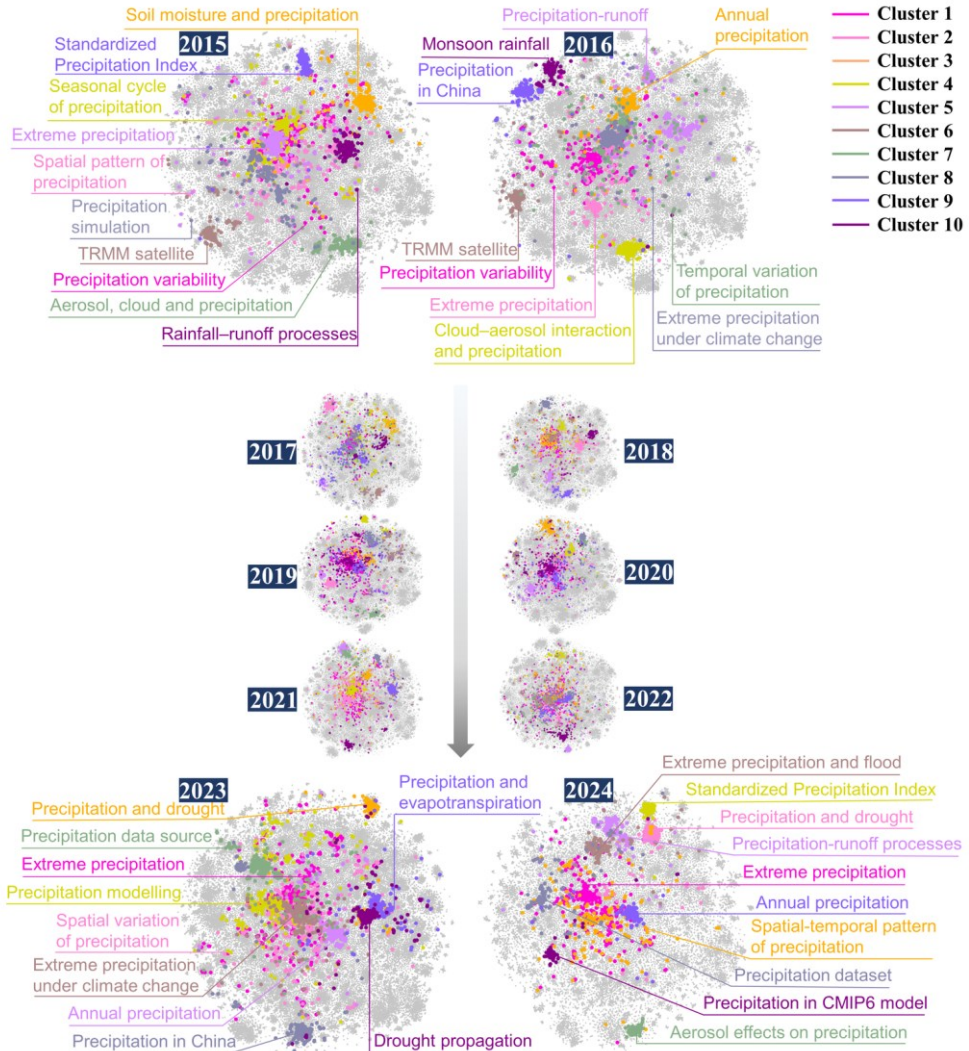


**Figure 5.** Taking “precipitation” as an example to illustrate sentence-level clustering. In this instance, sentences containing the words “precipitation” (case-insensitive) or “rain” (case-insensitive) were extracted, followed by the application of unsupervised clustering for each year. The sub-plot illustrates the dynamic research hotspots within the domain of precipitation from 2015 to 2024. Annually, approximately 130,000 scattered data points are recorded from 2015 to 2023, with this number decreasing to around 50,000 points in 2024 (up to June 2024). The analysis identified the top ten clusters, with “Cluster 1” encompassing the highest number of sentences, gradually decreasing to “Cluster 10”. The principal topics within each cluster are presented adjacent to the clusters, maintaining consistency through the use of a uniform color scheme. Due to layout constraints, the principal topics for years from 2017 to 2022 were not displayed.

Figure 5 presents the results of a clustering analysis applied to over 1.6 million precipitation-related sentences, extracted and analyzed on an annual scale. In 2015, the primary emphasis of research was on the temporal and spatial patterns of precipitation and the mechanisms of its formation. By contrast, by 2023 and 2024, the research focus had evolved toward extreme hydrological events (like extreme precipitation, droughts, and floods), the role of precipitation within the hydrosphere, and the effects of climate change on precipitation. This indicates that unsupervised clustering can effectively and automatically identify research hotspots and their trends over time.

### 3.3 Sentence-level sentiment analysis

The critical nature of the ongoing water crisis within the Earth-human system is clearly depicted in Figure 4. I further filtered all sentences containing “water resource” and subjected them to sentiment analysis using *go-emotion* language model. Following the removal of “neutral” sentiment, “approval” was the most frequently observed emotion, particularly in the context of discussions on groundwater management, extreme hydrological events, wastewater treatment, snow-glacier dynamics, and multidisciplinary investigations into water resource management (Figure 6). The analysis further demonstrated that “disappointment,” the second most common emotion, was prominent within conversations pertaining to agricultural drought, groundwater over-extraction, the increasing impact of population and economic expansion on water demand, water pollution, and the intensifying influence of climate change on water resources. While more than 500 records exhibited “optimism,” deeper examination revealed that this sentiment was frequently associated with two central topics: authors highlighting the significance of their studies and admissions that climate change could potentially worsen water-related problems (which would be more appropriately categorized as pessimism). The continued deterioration of water resources despite widespread research indicates a separation between research findings and policy implementation. In general, the overarching sentiment pertaining to water resources is negative, underscoring several critical challenges that necessitate prompt action.

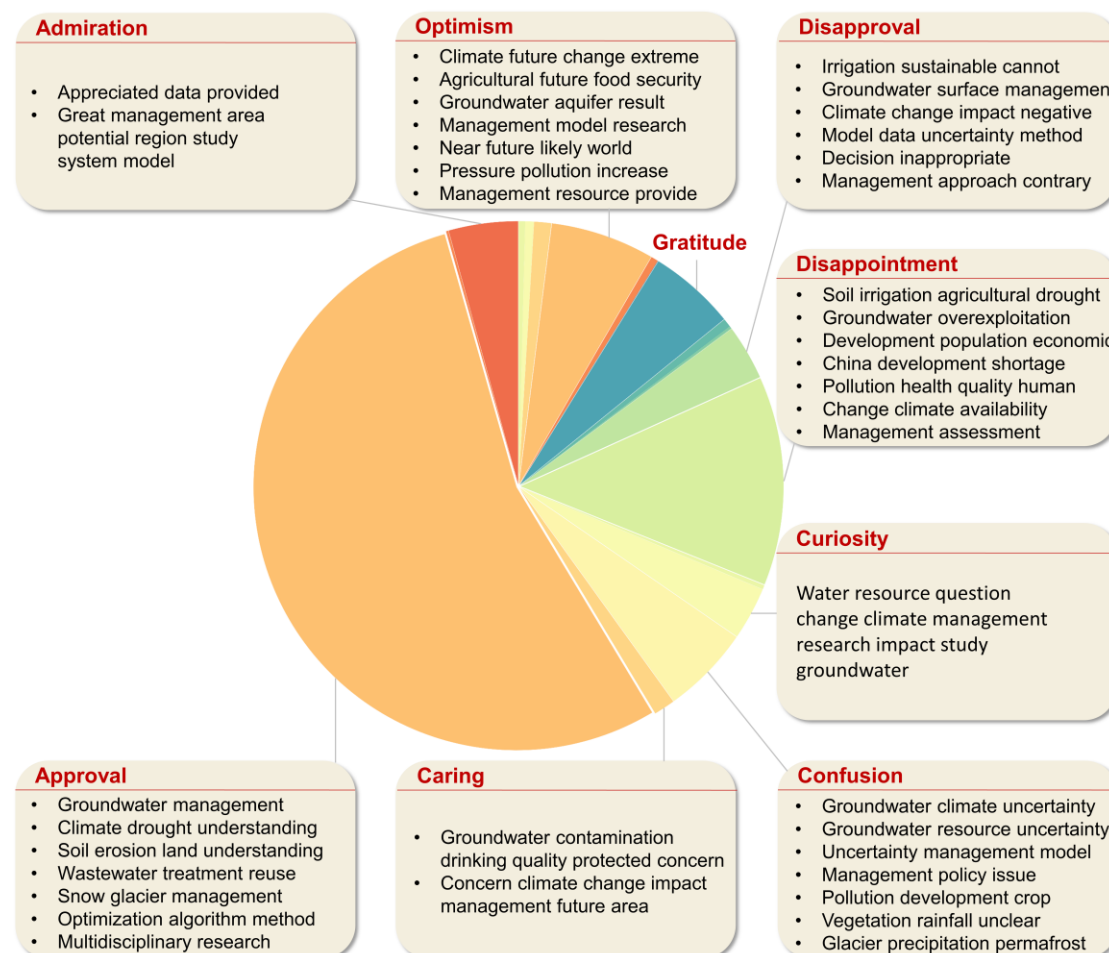


**Figure 6.** Illustration the application of sentence-level sentiment analysis by the *go-emotion* language model, using “water resource” (case-insensitive) as a case study. A total of 98,681 relevant sentences were extracted. Following this, emotional categories with more than 100 supporting sentences were filtered, while excluding neutral emotions. This procedure identified “approval” (4,787) and “disappointment” (1,133) as the most prevalent emotions. The “gratitude” category, primarily consisting of funding acknowledgements, was removed from further analyses. In the topic modeling by the *BERTopic* language model, the “curiosity” sentiment was consolidated into a single topic group. To maintain brevity, only the seven most prominent topic groups identified within the “approval,” “disappointment,” “optimism,” and “confusion” emotional categories are presented.

Furthermore, unsupervised clustering of all negatively-toned freshwater-related sentences (164,381 records in total) detected by the *Twitter-RoBERTa-base-sentiment-latest* language model yielded 40 distinct classes since 2015, coinciding with the introduction of SDGs (Figure 7a; Table S1). These clusters reveal that freshwater ecosystems are under severe stress from interconnected issues, including pollution, climate change, invasive species, overexploitation, and habitat loss, ultimately leading to biodiversity decline and ecosystem degradation. Freshwater scarcity is a worsening global problem due to rising demand, overuse, poor management, industrialization, erratic rainfall patterns, and climate change (e.g., Lazzin *et al.*, 2020; Sohi *et al.*, 2024). This problem is increasing in Africa, Asia, the Mediterranean, and on small islands (IPCC, 2022). Alarmingly, projections indicate that 75% of the world's population may face water scarcity by 2050 (Zhang *et al.*, 2022). Moreover, microplastics and diverse pollutants from industrial, agricultural, and urban activities contaminate freshwater globally, threatening water quality, aquatic life, and human health (e.g., Chen *et al.*, 2022).

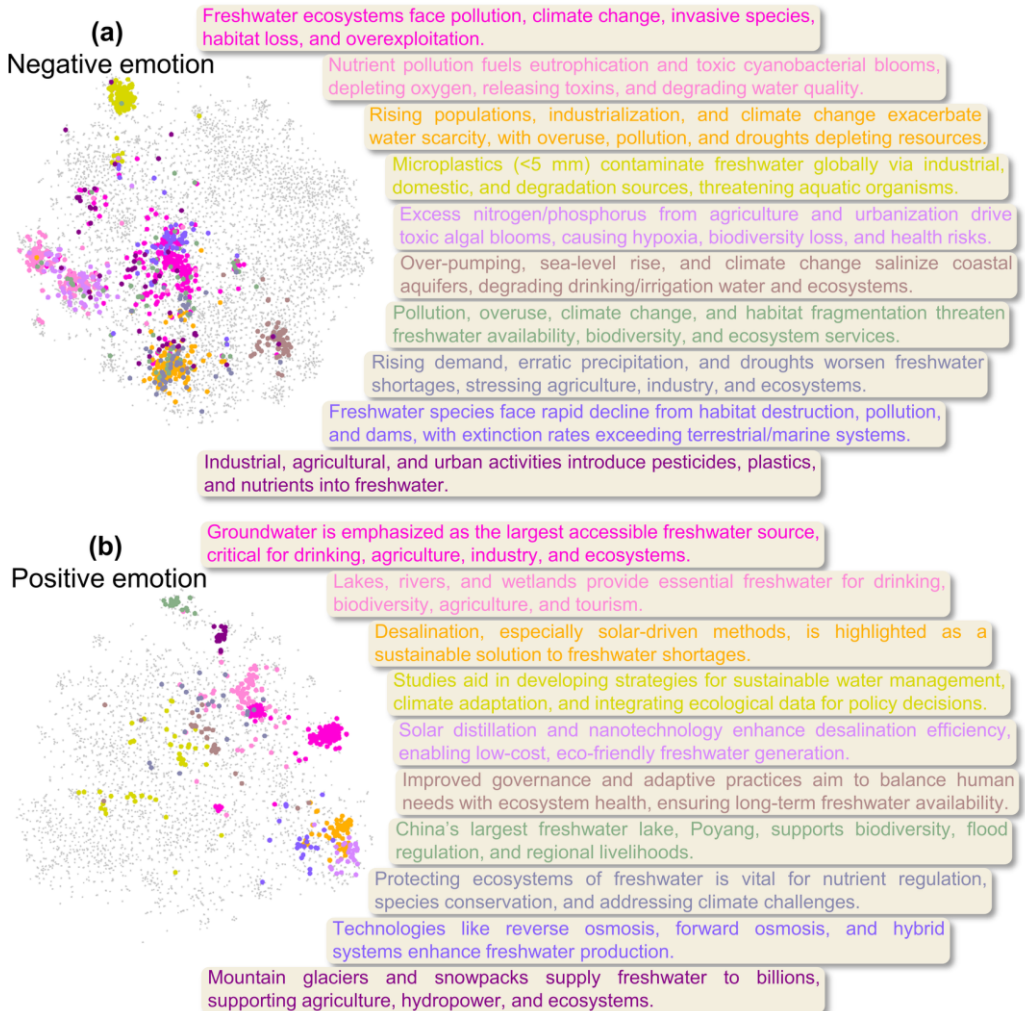


**Figure 7.** Top ten negative (a) and positive (b) emotions, which are detected by the *Twitter-RoBERTa-base-sentiment-latest* language model, in freshwater-related corpus since 2015. (a) is based on Table S1 and (b) is based on Table S2. The dispersed colored points in the scatter plot correspond directly to the colored LLM summarization on the right.

In contrast, analysis of the positively-toned freshwater corpus (Fig. 7b; Table S2) indicates that the importance of groundwater, lakes, rivers, wetlands, mountain glaciers, and snowpacks as sources of freshwater is frequently emphasized. Desalination technologies, particularly the solar distillation, the reverse osmosis, and the multi-effect distillation technologies, offer sustainable approaches to freshwater production (e.g., Forootan & Forootan, 2024). Furthermore, the efficiency of solar desalination system can be improved by energy storage materials including

nanotechnology and phase change materials (Jamil *et al.*, 2023). To achieve SDGs, sustainable freshwater management is essential.

## 4 Conclusion and discussion

Addressing the rapid expansion of literature, the need for effective interdisciplinary and transdisciplinary knowledge transfer, and the computation cost and the black-box nature posed by LLMs are critical for science community.

In this perspective, I establish a framework for a precise and cost-effective information acquisition in geoscience by integrating a range of MiniLMs with an extensive and meticulously curated corpus of high-quality sentences sourced from well-respected journals, thereby substantially enhancing the applicability of MiniLMs within geoscience. Through the creation of a corpus of approximately 77 million sentences, my work effectively demonstrates the capability of MiniLMs across three key downstream tasks: sentence-level semantic search, sentence-level unsupervised clustering, and sentence-level sentiment analysis.

Specifically, the semantic search facilitates the fact retrieval of a particular subdomain, efficiently converting a simple query into a detailed, professional, and often extensive summary when coupled with high-performance LLMs. Furthermore, this methodology aids in elucidating the inherent complexity, contradictoriness, and temporal evolution of given subjects across numerous disciplines. Importantly, it offers a cost-effective means of locating domain-specific knowledge with quantified data, potentially exceeding the reliability of powerful commercial tools like ChatGPT-4. In summary, precise and cost-effective information retrieval from geoscience literature can be achieved by: (1) curating a comprehensive collection of well-respected publications within a specific field; (2) segmenting these publications into high-quality individual sentences; and (3) utilizing freely available MiniLMs, such as *all-MiniLM-L6-v2*.

Unsupervised clustering can automatically identify similar patterns in sentences, aiding in the discovery of research priorities, conclusions, and limitations within a field or a discipline. This enables the formation of an overall disciplinary perspective, independent of subjective human judgment, by automatically capturing structured knowledge. However, unstructured knowledge, which is not captured by clustering, could be equally valuable in my opinion. These non-mainstream or marginalized viewpoints merit further re-evaluation and could ultimately drive the progress of the discipline.

Current sentiment analysis models, basically trained on social media data, this perspective remains exploratory in its application to the analysis of specific scientific issue. However, with a sufficiently large corpus, negative emotions detected by sentiment analysis can comprehensively expose the challenges, causes, and consequences associated with specific issues. This enables a thorough examination of critical issues facing the Earth-human system, such as climate change, water resource shortage, ecosystem degradation, pollution, agricultural security, and rapid urbanization and industrialization. As researchers, our more crucial task might be to seek potential solutions within crises. While positive emotions revealed by sentiment analysis can provide inspiration, they are unlikely to fully resolve these challenges.

Despite its strengths, the extraction of a high-quality corpus from PDFs is still subject to several limitations. The corpus is affected by fragmented sentences and words, exemplified by the misinterpretation of “significant” as “signifiant” due to typesetting inconsistencies. Furthermore, the correct handling of formulas remains a substantial challenge. Additionally, the necessity to uphold the copyright of the literature restricts this methodology to research-oriented uses within the science community. Also, limited by my background, the examples provided in this perspective are primarily focused on atmospheric sciences.

## 5 Using MiniLMs to validate LLMs

The current focus within the research community is largely directed toward LLMs. The escalating capabilities of LLMs, while largely facilitating knowledge exchange, might also significantly erode public confidence in knowledge creation. If LLMs were to dominate the interpretation of discourse within human civilization, what would remain of the unique value of humanity? In contrast, MiniLM offers individuals the capacity to filter and reorganize information, and even question the outputs of LLMs, offering high precision at a much lower computational cost. Moreover, leveraging the ancient Chinese wisdom of Yin-Yang (阴-阳) philosophy, such as through completely opposite prompts or sentiment analysis, it is relatively helpful to discover and understand the duality of things, and fully recognize the progress and limitations of the discipline.

Furthermore, a user-friendly sentence-level MiniLM-based search platforms provided by reputable publishers or groups would be invaluable, allowing different groups, regardless of their expertise level, to access relevant professional information. The increasing prevalence of open-access publishing suggests that authors might prioritize a broad attention. This raises another fundamental question: Is the value of academic papers measured by citation counts, or should they be considered a collective body of knowledge of human serving the common good? For Earth science researchers, what constitutes “scientific importance”? Is it primarily the health of our planet or the well-being of humanity? Despite the extensive body of research emerging from Earth science, the unprecedented rates of change in Earth system is still likely exceeding “safe” levels in several dimensions (Anenberg *et al.*, 2019; Rockström *et al.*, 2021). A more holistic approach is needed, one that transcends disciplinary boundaries and incorporates multi-dimensional perspectives. Research papers, representing the collective wisdom of Earth, environment, and space scientists, should be readily accessible to the public, policymakers, and even middle school students.

## Acknowledgements

The author would like to acknowledge the National Natural Science Foundation of China under Grant 42205074. I am deeply grateful to Pro. Michael Wysession for providing the opportunity to submit this work for review. I also extend my sincere appreciation to Pro. Yunyue Elita Li and the two anonymous reviewers for their insightful and constructive feedback.

## Data Availability Statement

A simplified procedure for utilizing MiniLM is available at Zhang (2025).

## Conflict of Interest

The author declares no conflicts of interest relevant to this study

## References

Anenberg, S. C., Dutton, A., Goulet, C., Swain, D. L., & van der Pluijm, B. (2019). Toward a resilient global society: Air, sea level, earthquakes, and weather. *Earth's Future*, 7, 854–864. <https://doi.org/10.1029/2019EF001242>

Bergen, K. J., Johnson, P. A., de Hoop, M. V. & Beroza, G. C. (2019). Machine learning for data-driven discovery in solid Earth geoscience. *Science*, 363, eaau0323. <https://doi.org/10.1126/science.aau0323>

Best, J. (2019). Anthropogenic stresses on the world's big rivers. *Nature Geoscience*, 12(1), 7–21. <https://doi.org/10.1038/s41561-018-0262-x>

Chen, H., Jia, Q., Sun, X., Zhou, X., Zhu, Y., Guo, Y., & Ye, J. (2022). Quantifying microplastic stocks and flows in the urban agglomeration based

on the mass balance model and source-pathway-receptor framework: Revealing the role of pollution sources, weather patterns, and environmental management practices. *Water Research*, 224, 119045. <https://doi.org/10.1016/j.watres.2022.119045>

Cui, H. (2021). Inside out: deep carbon linked to deep-time carbon cycle. *Science Bulletin*, 66(18), 1822–1824. <https://doi.org/10.1016/j.scib.2021.06.001>

Demszky, D., Movshovitz-Attias, D., Ko, J., Cowen, A., Nemadé, G., & Ravi, S. (2020). GoEmotions: A dataset of fine-grained emotions. arXiv preprint arXiv:2005.00547.

Forootan, M. M., & Ahmadi, A. (2024). Machine learning-based optimization and 4E analysis of renewable-based polygeneration system by integration of GT-SRC-ORC-SOFC-PEME-MED-RO using multi-objective grey wolf optimization algorithm and neural networks. *Renewable and Sustainable Energy Reviews*, 200, 114616. <https://doi.org/10.1016/j.rser.2024.114616>

Foroumandi, E., Moradkhani, H., Sanchez-Vila, X., Singha, K., Castelletti, A., & Destouni, G. (2023). ChatGPT in hydrology and Earth sciences: Opportunities, prospects, and concerns. *Water Resources Research*, 59, e2023WR036288. <https://doi.org/10.1029/2023WR036288>

Gougherty, A. V., & Clipp, H. L. (2024). Testing the Reliability of an AI-Based Large Language Model to Extract Ecological Information From the Scientific Literature. *NPJ Biodiversity*, 3, 1–5. <https://doi.org/10.1038/s44185-024-00043-9>

IPCC. (2022). In H. O. Pörtner, D. C. Roberts, M. Tignor, E. S. Poloczanska, K. Mintenbeck, A. Alegría, et al. (Eds.), Climate change 2022: Impacts, adaptation, and vulnerability. Cambridge University Press. <https://dx.doi.org/10.1017/9781009325844>

Jablonka, K. M., Schwaller, P., Ortega-Guerrero, A., & Smit, B. (2024). Leveraging large language models for predictive chemistry. *Nature Machine Intelligence*, 6, 161–169. <https://doi.org/10.1038/s42256-023-00788-1>

Jamil, F., Hassan, F., Shoeibi, S., & Khiadani, M. (2023). Application of advanced energy storage materials in direct solar desalination: a state of art review. *Renewable and Sustainable Energy Reviews*, 186, 113663. <https://doi.org/10.1016/j.rser.2023.113663>

Lazin, R., Shen, X., Koukoula, M., & Anagnostou, E. (2020). Evaluation of the hyper-resolution model-derived water cycle components over the upper Blue Nile Basin. *Journal of Hydrology*, 590, 125231. <https://doi.org/10.1016/j.jhydrol.2020.125231>

Li, Y. E., O'Malley, D., Beroza, G., Curtis, A., & Johnson, P. (2023). Machine learning developments and applications in Solid-Earth geosciences: Fad or future? *Journal of Geophysical Research: Solid Earth*, 128, e2022JB026310. <https://doi.org/10.1029/2022JB026310>

Kononova, O., He, T., Huo, H., Trewartha, A., Olivetti, E. A., & Ceder, G. (2021). Opportunities and challenges of text mining in materials research. *Isclimate*, 24(3). <https://doi.org/10.1016/j.iscli.2021.102155>

M. Bran, A., Cox, S., Schilter, O., Baldassari, C., White, A. D., & Schwaller, P. (2024). Augmenting large language models with chemistry tools. *Nature Machine Intelligence*, 6(5), 525–535. <https://doi.org/10.1038/s42256-024-00832-8>

Meng, R., Liu, Y., Joty, S. R., Xiong, C., Zhou, Y., & Yavuz, S. (2024). Sfrembedding-mistral: enhance text retrieval with transfer learning. Salesforce AI Research Blog, 3, 6.

Nielsen, J. Ø., & D'haen, S. A. L. (2014). Asking about climate change: Reflections on methodology in qualitative climate change research published in global environmental change since 2000. *Global Environmental Change*, 24, 402–409. <https://doi.org/10.1016/j.gloenvcha.2013.10.006>

Ott, S., Hebenstreit, K., Liévin, V., Hother, C. E., Moradi, M., Mayrhauser, M., Robert, P., Ole, W., & Samwald, M. (2023). ThoughtSource: A central hub for large language model reasoning data. *Scientific Data*, 10, 528. <https://doi.org/10.1038/s41597-023-02433-3>

Ramachandran, R., & Bugbee, K. (2025). Balancing practical uses and ethical concerns: The role of large language models in scientific research. *Perspectives of Earth and Space Scientists*, 6, e2024CN000258. <https://doi.org/10.1029/2024CN000258>

Reimers, N., & Gurevych, I. (2019a). Sentence-bert: Sentence embeddings using siamese bert-networks. arXiv preprint arXiv:1908.10084.

Reimers, N., & Gurevych, I. (2019b). Sentence Transformers documentation. Accessed at 21 July 2025. [https://www.sbert.net/docs/sentence\\_transformer/pretrained\\_models.html](https://www.sbert.net/docs/sentence_transformer/pretrained_models.html)

Ren, Y., Yu, H., Huang, J., Peng, M., & Zhou, J. (2024). The projected response of the water cycle to global warming over drylands in East Asia. *Earth's Future*, 12, e2023EF004008. <https://doi.org/10.1029/2023EF004008>

Rockström, J., Gupta, J., Lenton, T. M., Qin, D., Lade, S. J., Abrams, J. F., et al. (2021). Identifying a safe and just corridor for people and the planet. *Earth's Future*, 9, e2020EF001866. <https://doi.org/10.1029/2020EF001866>

Sohi, H. Y., Zahraie, B., Dolatabadi, N., & Zebarjad, F. (2024). Application of VIC-WUR model for assessing the spatiotemporal distribution of water availability in anthropogenically-impacted basins. *Journal of Hydrology*, 637, 131365. <https://doi.org/10.1016/j.jhydrol.2024.131365>

Tshitoyan, V., Dagdelen, J., Weston, L., Dunn, A., Rong, Z., Kononova, O., Persson, K. A., Ceder, G., & Jain, A. (2019). Unsupervised word embeddings capture latent knowledge from materials science literature. *Nature*, 571(7763), 95–98. <https://doi.org/10.1038/s41586-019-1335-8>

UN-Water. (2021). Summary Progress Update 2021: SDG 6 — Water and sanitation for all, Geneva. <https://www.unwater.org/publications/sdg-6-progress-reports>

Vance, T. C., Huang, T., & Butler, K. A. (2024). Big data in Earth science: Emerging practice and promise. *Science*, 383(6688), eadh9607. <https://doi.org/10.1126/science.adh9607>

Vörösmarty, C. J., McIntyre, P. B., Gessner, M. O., Dudgeon, D., Prusevich, A., Green, P., Glidden, S., Bunn, S. E., Sullivan, C. A., Reidy Liermann, C., & Davies, P. (2010). Global threats to human water security and river biodiversity. *Nature*, 467(7315), 555–561. <https://doi.org/10.1038/nature09440>

Wu, H., Yang, Q., Liu, J., & Wang, G. (2020). A spatiotemporal deep fusion model for merging satellite and gauge precipitation in China. *Journal of Hydrology*, 584, 124664. <https://doi.org/10.1016/j.jhydrol.2020.124664>

Zhang, J. (2025). Tips for MiniLM [Dataset]. Retrieved from <https://doi.org/10.6084/m9.figshare.29616506.v1>

Zhang, W., Huang, J., Zhang, T., & Tan, Q. (2022). A risk-based stochastic model for supporting resources allocation of agricultural water-energy-food system under uncertainty. *Journal of Hydrology*, 610, 127864. <https://doi.org/10.1016/j.jhydrol.2022.127864>

## Supporting Information

**Table S1.** Unsupervised clustering was performed on negative emotions in freshwater-related corpus since 2015. Sentences were embedded using PSTM\_4, with clustering parameters set to a minimum cluster count of 10 and a minimum similarity score of 0.85. Cluster topics and summaries were automatically generated by the DeepSeek LLM, using the prompt: “Please find the topic within 10 words and summarize the text file within 50 words.”

Cluster	Topic	Summary
0	<b>Threats to freshwater ecosystems: pollution, climate change, habitat loss</b>	Freshwater ecosystems face pollution, climate change, invasive species, habitat loss, and overexploitation, driving biodiversity decline, hypoxia, and ecosystem service degradation. Urgent action is needed to mitigate these interconnected stressors threatening aquatic life and human well-being.
1	<b>Eutrophication and harmful algal blooms threatening freshwater ecosystems</b>	Nutrient pollution fuels eutrophication and toxic cyanobacterial blooms, depleting oxygen, releasing toxins, and degrading water quality. These blooms harm biodiversity, disrupt food chains, and jeopardize drinking water, fisheries, and human health globally.
2	<b>Freshwater scarcity driven by population growth and climate change</b>	Rising populations, industrialization, and climate change exacerbate water scarcity, with overuse, pollution, and droughts depleting resources. By 2025, half the global population may face water stress, threatening agriculture, health, and socioeconomic stability.
3	<b>Microplastic pollution in freshwater ecosystems</b>	Microplastics (<5 mm) contaminate freshwater globally via industrial, domestic, and degradation sources, threatening aquatic organisms through ingestion, toxin adsorption, and ecosystem disruption, with risks to biodiversity and human health via food chains.
4	<b>Nutrient pollution causing harmful algal blooms</b>	Excess nitrogen/phosphorus from agriculture and urbanization drive toxic algal blooms in freshwater, causing hypoxia, biodiversity loss, and health risks via contaminated water and seafood.
5	<b>Seawater intrusion threatening coastal freshwater resources</b>	Over-pumping, sea-level rise, and climate change salinize coastal aquifers, degrading drinking/irrigation water and ecosystems, exacerbating scarcity in densely populated regions.
6	<b>Multiple stressors degrading freshwater sustainability</b>	Pollution, overuse, climate change, and habitat fragmentation threaten freshwater availability, biodiversity, and ecosystem services, necessitating urgent integrated management.
7	<b>Climate change and population growth intensifying water scarcity</b>	Rising demand, erratic precipitation, and droughts worsen freshwater shortages, stressing agriculture, industry, and ecosystems, particularly in arid regions.
8	<b>Biodiversity loss in freshwater ecosystems</b>	Freshwater species face rapid decline from habitat destruction, pollution, and dams, with extinction rates exceeding terrestrial/marine systems, disrupting ecological functions.
9	<b>Anthropogenic pollutants degrading freshwater quality</b>	Industrial, agricultural, and urban activities introduce pesticides, plastics, and nutrients into freshwater, compromising ecosystems, human health, and water security.
10	<b>Toxic cyanobacterial blooms in freshwater systems</b>	Nutrient-driven cyanobacteria blooms release toxins (e.g., microcystins), endangering drinking water, aquatic life, and human health through oxygen depletion and poisoning.
11	<b>Global freshwater scarcity crisis</b>	Population growth, industrialization, and pollution drive global freshwater shortages, affecting billions. Projections indicate 75% of people may face scarcity by 2050, threatening food, energy security, and ecosystems.
12	<b>Human impacts on freshwater biodiversity</b>	Urbanization, agriculture, and pollution degrade freshwater ecosystems, causing biodiversity loss and population declines in invertebrates and fish through habitat alteration and contamination.
13	<b>Freshwater salinization risks</b>	Rising salinity from road salts, wastewater, and agriculture harms aquatic life, mobilizes contaminants, and threatens drinking water, biodiversity, and ecosystem services globally.
14	<b>Climate change threats to freshwater</b>	Warming temperatures, altered flow regimes, and stratification degrade freshwater ecosystems, stressing fish populations and increasing risks of hypoxia and harmful algal blooms.
15	<b>Coastal aquifer seawater intrusion</b>	Over-pumping and sea-level rise cause saltwater intrusion into coastal aquifers, contaminating freshwater supplies, harming agriculture, and endangering drinking water quality.
16	<b>Emerging contaminants in freshwater</b>	Microplastics, pharmaceuticals, and pollutants accumulate in freshwater ecosystems, with poorly understood ecological and health risks due to limited research and monitoring.
17	<b>Depletion of freshwater resources</b>	Urbanization, climate change, and rising demand deplete freshwater availability, exacerbating water stress and threatening sustainability in arid and densely populated regions.
18	<b>Nutrient-driven freshwater eutrophication</b>	Excess phosphorus and nitrogen from agriculture and wastewater fuel harmful algal blooms, degrading water quality, causing hypoxia, and disrupting aquatic ecosystems globally.
19	<b>Irrigation strains on freshwater</b>	Agricultural expansion intensifies freshwater extraction, depleting aquifers and rivers, worsening scarcity, and heightening competition in water-stressed regions.
20	<b>Climate-driven saltwater intrusion</b>	Sea-level rise, droughts, and over-pumping accelerate saltwater intrusion into coastal freshwater, contaminating supplies and disrupting ecosystems and human

		livelihoods.
21	<b>Industrial pollution and heavy metals degrading freshwater resources</b>	Industrial activities and heavy metals (e.g., $Hg^{2+}$ ) contaminate freshwater, causing scarcity and threatening ecosystems, particularly in developing nations.
22	<b>Freshwater biodiversity loss exceeds marine/terrestrial ecosystems</b>	Freshwater species face rapid declines due to habitat loss, pollution, and invasive species, with extinction rates surpassing marine/terrestrial environments.
23	<b>Agricultural runoff and nitrogen pollution harm freshwater quality</b>	Nitrogen from agriculture causes eutrophication, oxygen depletion, and ecosystem damage in freshwater, impacting drinking water and coastal areas.
24	<b>Freshwater scarcity due to supply-demand mismatches and overuse</b>	Over-extraction, droughts, and poor infrastructure exacerbate freshwater shortages, stressing regions like the YRB and arid zones.
25	<b>Sea-level rise contaminates freshwater via saltwater intrusion</b>	Coastal aquifers face salinization from rising seas, threatening freshwater availability for ecosystems, agriculture, and human consumption.
26	<b>Pesticide pollution disrupts freshwater biodiversity</b>	Agricultural pesticides harm zooplankton and fish, reducing biodiversity and causing ecological risks, particularly in vulnerable regions.
27	<b>Climate change intensifies freshwater system instability</b>	Extreme weather and pollution worsen freshwater scarcity, eutrophication, and ecosystem health, challenging global water security.
28	<b>Excess phosphorus drives freshwater eutrophication globally</b>	Phosphorus from agriculture and industry triggers algal blooms, degrading water quality and causing economic losses in freshwater systems.
29	<b>Toxic contaminants threaten freshwater ecosystems and human health</b>	MPs, heavy metals, and pharmaceuticals bioaccumulate, harming aquatic life and human health through toxicological effects.
30	<b>Microplastics severely impact freshwater ecosystems</b>	MPs disrupt organisms, nutrient cycles, and food webs in freshwater, with risks from additives and cross-system contamination.
31	<b>Agriculture's high freshwater consumption threatens sustainability</b>	Agriculture uses 50-80% of global freshwater, causing scarcity, ecosystem stress, and competition with municipal/environmental needs. Irrigation-driven depletion, pollution, and climate change exacerbate risks to sustainable food production and water security.
32	<b>Data gaps hinder freshwater dynamics understanding</b>	Limited in-situ data, sparse monitoring, and poor spatial-temporal resolution obscure freshwater storage quantification, seasonal variability, and ecological impacts. Remote sensing and modeling face uncertainties, hampering policy and management decisions.
33	<b>Freshwater influx weakens Atlantic Ocean circulation (AMOC)</b>	Increased freshwater from ice melt reduces North Atlantic Deep Water formation, weakening Atlantic Ocean circulation. This disrupts heat transport, causing regional cooling (e.g., "warming hole") and amplifying climate feedbacks.
34	<b>Plastic pollution endangers freshwater ecosystems globally</b>	Plastics infiltrate rivers and lakes, harming biodiversity via entanglement, toxicity, and food chain contamination. Agricultural runoff and poor waste management exacerbate pollution, threatening water quality and human health.
35	<b>Freshwater ecotoxicity and eutrophication dominate environmental impacts</b>	Key impact categories include freshwater eutrophication, ecotoxicity, and human toxicity. Agriculture and industry drive nutrient pollution, chemical contamination, and resource depletion, degrading aquatic ecosystems.
36	<b>Multiple stressors threaten freshwater biodiversity and ecosystems</b>	Pollution, warming, invasive species, and habitat loss synergistically harm freshwater organisms. Mollusks and invertebrates face high extinction risks, disrupting food webs and ecosystem resilience.
37	<b>Climate change intensifies droughts and freshwater scarcity</b>	Rising temperatures and erratic rainfall reduce water availability, exacerbating droughts. Regions like the Mediterranean and small islands face agricultural losses, ecosystem collapse, and water conflicts.
38	<b>Eutrophication plagues China's major freshwater lakes</b>	Taihu, Chaohu, and Poyang Lakes suffer algal blooms and pollution from agriculture, industry, and urbanization. Nutrient runoff degrades water quality, threatening drinking supplies and biodiversity.
39	<b>Small islands face acute freshwater scarcity and salinity</b>	Limited groundwater, climate vulnerability, and overuse cause water shortages in island communities. Saltwater intrusion and droughts jeopardize ecosystems and human survival, requiring urgent sustainable management.

**Table S2.** Similar to Tab. S1 but for the positive emotion in freshwater-related corpus.

Cluster	Topic	Summary
0	<b>Groundwater as the primary global freshwater resource</b>	Groundwater is emphasized as the largest accessible freshwater source, critical for drinking, agriculture, industry, and ecosystems. It supports billions of people and global food security, with studies citing its irreplaceable role in sustaining human needs and environmental stability.
1	<b>Lakes and rivers as vital freshwater ecosystems</b>	Lakes, rivers, and wetlands provide essential freshwater for drinking, biodiversity, agriculture, and tourism. They offer ecosystem services like flood control, nutrient cycling, and cultural value, supporting millions globally while

		balancing ecological and socioeconomic needs.
2	<b>Desalination technologies addressing freshwater scarcity</b>	Desalination, especially solar-driven methods, is highlighted as a sustainable solution to freshwater shortages. Innovations like reverse osmosis and hydrate-based processes aim to efficiently convert seawater into potable water, particularly for arid regions.
3	<b>Research insights into freshwater ecosystem management</b>	Studies focus on understanding freshwater systems, pollution control, and biodiversity conservation. Findings aid in developing strategies for sustainable water management, climate adaptation, and integrating ecological data for policy decisions.
4	<b>Solar-driven desalination advancements for freshwater production</b>	Solar distillation and nanotechnology enhance desalination efficiency, enabling low-cost, eco-friendly freshwater generation. Innovations like interfacial evaporation and phase-change materials improve productivity, addressing water scarcity in energy-limited regions.
5	<b>Sustainable management of freshwater resources</b>	Strategies emphasize holistic conservation, biodiversity protection, and stakeholder collaboration. Improved governance and adaptive practices aim to balance human needs with ecosystem health, ensuring long-term freshwater availability.
6	<b>Poyang Lake's ecological and economic significance</b>	China's largest freshwater lake, Poyang, supports biodiversity, flood regulation, and regional livelihoods. Studies highlight its role in carbon sequestration, fisheries, and as a Ramsar wetland critical to the Yangtze River Basin.
7	<b>Freshwater ecosystems' role in global sustainability</b>	Freshwater environments sustain biodiversity, carbon cycles, and human well-being. Protecting these ecosystems is vital for nutrient regulation, species conservation, and addressing climate challenges through integrated socio-ecological approaches.
8	<b>Sustainable freshwater production through energy-efficient technologies</b>	Technologies like reverse osmosis, forward osmosis, and hybrid systems enhance freshwater production, improve energy efficiency, reduce CO <sub>2</sub> emissions, and decrease fossil fuel reliance, addressing future water demands sustainably while promoting renewable energy integration.
9	<b>Glaciers and snowpacks as vital freshwater sources</b>	Mountain glaciers and snowpacks supply freshwater to billions, supporting agriculture, hydropower, and ecosystems in regions like the Himalayas, Tibetan Plateau, and Andes, crucial for arid areas and downstream populations.
10	<b>Methane dynamics in freshwater ecosystems and climate impact</b>	Freshwater ecosystems significantly contribute to global methane emissions, with temperature and eutrophication influencing CH <sub>4</sub> production. Improved models are needed to assess their role in greenhouse gas budgets and climate change.



**Figure S1.** A software demonstration illustrates semantic searching capabilities within atmospheric science literature. The software was run on a laptop equipped with an Intel® Core™ i7-10750H CPU @ 2.60GHz, 64GB of memory, and an NVIDIA Quadro P620 GPU. The right panel replicates a query generated by ChatGPT-4: “The wind speed decrease m/s to m/s under climate change.”

The top-matched sentences, identified by the PSTM\_3 model, are highlighted in orange, with the corresponding relevance score indicated numerically. Contextual sentences preceding and following the matched segments are displayed in black, with blue annotations denoting the original reference. An “OPEN” button facilitates direct access to the original publication in PDF format. In this instance, sentence-based searching yielded results quantifying wind speed decreases. Furthermore, the search highlighted discrepancies in wind speed trends under climate change as reported by different reanalysis products. Due to display constraints, only the highest-ranked sentences are presented. In contrast, ChatGPT-4 suggested consulting publications in journals such as *Geophysical Research Letters* and *Nature Climate Change*, offering a broader but less specific result.

You Wind speed increased from m/s to m/s under climate change  
∅

 Okay, again, I need the numbers to complete the sentence and offer any meaningful analysis. Please provide the "from" and "to" wind speeds in m/s.

For example:

"Wind speed increased from 5 m/s to 7 m/s under climate change."

Once you give me the numbers, I can complete the sentence and potentially offer some context or related information.

**Figure S2.** Conversely, applying the query “Wind speed increased from m/s to m/s under climate change” to the semantic search software reveals substantial evidence indicating an increase in wind speed (near-surface winds or jet stream) within historical research. This includes quantified data and associated mechanisms. In contrast, ChatGPT-4 was unable to retrieve quantitative data pertaining to wind speed increases.

The horizontal wavelength of gravity waves is km	
0.88: An upper radiation condition is applied to reduce the reflection of energy and to prevent spurious noise buildup near the top boundary. <b>Gravity waves found in this study are approximately 15–300 km in horizontal wavelength.</b> Because of the 3-km resolution of the smallest nest, wavelength components smaller than about 15 km are damped by the numerical dissipation.	
IAS-2003-Daily and Subdaily Wind and Divergence Variations Observed by a Shipborne Doppler Radar off the Southeastern Coast of Sumatra <a href="#">OPEN</a>	
0.84: There was an approximate phase locking of the semidiurnal variation with the diurnal variation in the wind and divergence fields. <b>The gravity waves displayed horizontal wavelengths of 50–60 km and periods of 1–3 h.</b> The precipitation propagated offshore, in phase with the density current and gravity waves.	
IAS-2003-Daily and Subdaily Wind and Divergence Variations Observed by a Shipborne Doppler Radar off the Southeastern Coast of Sumatra <a href="#">OPEN</a>	
0.82: Figures 12a and 12b indicate the existence of oscillations both in the cross-coast wind and in the vertical motion field. <b>Based on the vertical motion, the horizontal wavelength of the gravity wave was approximately 50–60 km.</b> Figure 13a indicates the existence of oscillations between 1400 and 1600 LT daily.	
IAS-2003-Daily and Subdaily Wind and Divergence Variations Observed by a Shipborne Doppler Radar off the Southeastern Coast of Sumatra <a href="#">OPEN</a>	
0.81: The effect is significant when the differential vertical motions have scales of the diameter of the area subtended by the radar beam, which at a height of 2–3 km is (cid:21)–1.5 km. <b>It seems unlikely that gravity waves would have horizontal wavelengths as short as this.</b> Time series for IOP2 of the mean square amplitude of each wind component in the height range 2–2.5 km are provided in Figure 7.	
IGRA-2004-VHF profiler observations of winds and waves in the troposphere during the Darwin Acme Wave Experiment DAWEX <a href="#">OPEN</a>	
0.81: The gravity waves propagate behind the eastward moving subtropical jet in a manner resembling the bow waves from a ship. <b>The two gravity waves have similar horizontal wavelength of about 262 km.</b> The upward propagating gravity wave has shorter vertical wavelength and higher intrinsic frequency in the stratosphere compared with the downward propagating gravity waves in the troposphere, probably because of larger background wind speeds and larger static stability in the stratosphere.	
IGRA-2004-General aspects of a T111L26 middle atmosphere general circulation model <a href="#">OPEN</a>	
0.80: Also shown on this plot are contours of the total horizontal wind speed, showing the location of the jet stream (>50 m/s) below 10 km altitude. <b>The vertical wavelength of the inertia-gravity wave is approximately 1.5 km.</b> As a wave approaches a critical level its vertical wavelength approaches zero, leading to instability and turbulence.	
GRL-2002-Gravity wave interactions around the jet stream <a href="#">OPEN</a>	
0.80: Although the theoretical results slightly overestimate the periods, the observed periods are generally in agreement with the theoretical dispersion relation under the windless assumption. <b>Additionally, according to Yue et al [2009], the theoretical horizontal wavelength <math>\lambda_h</math> of gravity wave is expressed as a function of horizontal radius and propagation time <math>\Delta t</math> as (cid:5) (cid:6)3=2 <math>\lambda_h \sqrt{2\pi R_2} \Delta t \sqrt{2\pi R_2} \Delta t</math> (3)</b> Figure 5d shows the theoretical relationship between the horizontal wavelengths and the radiiuses for each of the different propagation times (colored solid curves). The propagation times are estimated from the sources to the 200 km altitude based on the reversed ray tracing technique.	
GRL-2017-Cosmic ray ionospheric disturbances triggered by the launch of a SpaceX Falcon 9 rocket <a href="#">OPEN</a>	
0.79: We firstly applied the multi-channel maximum entropy method to the temperature profile triples based on the favorable conditions of satellite flight between year 2006 and 2007 after COSMIC launch, and analyzed the three-dimensional properties of GWs. <b>The latitudinal and seasonal distribution of horizontal wavelengths of gravity waves were obtained.</b> The momentum fluxes showed the maximum in the summertime subtropics and the wintertime high latitudes, which revealed possible convective sources in the summertime subtropics and mountain waves expected to occur in the winter jet region in the winter hemisphere high latitudes.	
GRL-2021-Three-Dimensional Analysis of Global Gravity Waves Based on COSMIC Multi-Satellite Observations <a href="#">OPEN</a>	
0.79: The parameters are estimated for the lower stratosphere (30–80 hPa), where the vertical wind shear of the polar night jet is small. <b>These gravity waves have short horizontal wavelengths, although the wavelengths remain substantially longer than the minimum resolved horizontal wavelength of the GCM (cid:4)188 km.</b> The gravity waves have small zonal phase speeds relative to the ground ( $j_{ex} < 1.8$ m s (cid:1)1) and high intrinsic frequencies ( $j_{\theta}^2/w_j < 0.15$ ).	
IGRA-2008-General aspects of a T211L26 middle atmosphere general circulation model <a href="#">OPEN</a>	
0.79: Note that different wave spectra are included due to different data resolutions used in these studies. <b>Gravity waves with periods of ~1–6 hr and vertical wavelengths of 2–30 km are included in the study of Yamashita et al whereas Kaifler et al put more emphasis on waves with periods longer than 2 hr and vertical wavelengths of ~4–20 km.</b> In this study, we include waves with periods of ~2–11 hr and vertical wavelengths of ~2–30 km.	
IGRA-2018-Lidar Observations of Stratospheric Gravity Waves From 2011 to 2015 in McMurdo 77.54°S 166.09°E Antarctica 2. Potential Energy Densities Latitudinal Distributions and Seasonal Variations <a href="#">OPEN</a>	
0.78: The seasonal variation seen over Patagonia was similar to that over the Falkland Islands, which are at the same latitude as our stations, unlike the Rothera station. <b>Parameters that characterized the gravity waves—the vertical and horizontal wavelengths, intrinsic period, and vertical and horizontal directions of propagation—were calculated as follows.</b> The observed vertical profiles of temperature, zonal wind, and meridional wind fluctuations over an altitude range of $\pm 0.5$ km for a given altitude grid were fitted to sinusoidal curves by least squares; the amplitude and phase were adjusted, and the vertical wavelength was fixed.	
IGRA-2018-Characteristics of Atmospheric Wave-Driven Luminous Observed by Ozoneondes at the Southern Tip of South America <a href="#">OPEN</a>	
0.78: Small-scale gravity waves (GWs) with horizontal wavelengths of tens up to several hundred kilometers are not resolved in general circulation models (GCMs) and hence need to be parameterized. <b>In addition to the wide range of horizontal scales, gravity waves have vertical wavelengths ranging from a few to a few tens of kilometers and periods ranging from several minutes to several hours.</b> Gravity waves are generated by a variety of sources including orography (eg., Lilly and Kennedy 1973; Do 1999), convection (eg., Dewan et al 1998; Piani and Durran 2001), and geostrophic adjustment in regions of baroclinic instability (eg., O’ Sullivan and Dunkerton 1995; Zhang 2004).	
JAS-2010-Toward a Physically Based Gravity Wave Source Parameterization in a General Circulation Model <a href="#">OPEN</a>	
0.78: Nonmigrating tides propagate their phases in a direction away from either of the two continents, which are located at $\sim 60^{\circ}\text{W}$ (South America) and $\sim 30^{\circ}\text{E}$ (Africa). <b>This is consistent with horizontal propagation characteristics of gravity waves.</b> Note that west and eastward propagating waves correspond to the west and eastward tilting waves in Figure 2, respectively.	
IGRA-2015-Three-dimensional structure of tropical nonmigrating tides in a high-vertical-resolution general circulation model <a href="#">OPEN</a>	
0.78: While this certainly does not prove that the waves present during our PMSE observations had exactly the same properties, we may still use a horizontal wavelength of about 20 km in order to estimate the order of magnitude effect of wave broadening on our own spectral observations. <b>Finally, we used the dispersion relation for high-frequency gravity waves [e.g., Fritts and Alexander, 2003, equation (30)] to derive a corresponding vertical wavelength.</b> Here, we show the altitude profiles of all relevant terms in equation (1).	
IGRA-2010-Morphological parameters of mesospheric ice clouds derived from calibrated observations of polar mesospheric noctilucent clouds at Brigg wavelength of 28 and 30 cm <a href="#">OPEN</a>	
0.78: Consequently, our results emphasize the importance of semidiurnal wind variation in modulating daily kinematic structure and precipitation off the southwestern coast of Sumatra. <b>Because of their horizontal wavelengths of 50–60 km and periods of 1–3 h, the observed gravity waves are fundamentally mesoscale in character (Uccellini and Koch 1987; Koch and O’Handley 1997).</b> This result is in contrast to the diurnal gravity waves illustrated in previous studies on the western and southwestern coasts of Sumatra (Mori et al 2004; Love et al 2011; Yokoi et al 2017; Wei et al 2020; Bai et al 2021).	
IAS-2023-Daily and Subdaily Wind and Divergence Variations Observed by a Shipborne Doppler Radar off the Southeastern Coast of Sumatra <a href="#">OPEN</a>	
0.77: The dominant horizontal wavelength decreases with increasing latitude in both the troposphere and lower stratosphere, with larger values in the lower stratosphere. <b>The latitudinal variation of horizontal wavelength is consistent with previous studies, and is shown to be a straightforward result of the gravity wave dispersion relation.</b> The troposphere–stratosphere differences are caused mostly by the differences in the stability characteristics in the two different regions.	
IAS-2009-Spatial and Temporal Variation of Gravity Wave Parameters: Part I Latitude Frequency Wavelength and Vertical Propagation Direction <a href="#">OPEN</a>	
0.77: However, even in the full moisture case, eastward momentum flux is much smaller than westward momentum flux. <b>Our experiments show the different behaviors of gravity wave spectral characteristics between gravity waves with short and medium horizontal scales.</b> For the short	

You

The horizontal wavelength of gravity waves is km

0

0.77

The horizontal wavelength of gravity waves can vary greatly, ranging from millimeters to hundred of kilometers.

Therefore, the statement “The horizontal wavelength of gravity waves is km” is incomplete without specifying the range of kilometers being referred to.

To make the statement more accurate, you could say something like:

- “The horizontal wavelength of some gravity waves is on the order of kilometers.”
- “The horizontal wavelength of gravity waves can be in the kilometers range.”
- “Gravity waves can have horizontal wavelengths reaching kilometers.”

However, without more information, it's impossible to give a precise answer.

0

**Figure S3.** A simple query, “The horizontal wavelength of gravity waves is km” was conducted. The software generated a range of gravity wave parameters, including vertical and horizontal wavelengths, as well as wave periods. In contrast, ChatGPT-4 stated that wavelengths range from millimeters to hundreds of kilometers, a conclusion obviously inconsistent with current research.



the turbulence dissipation rate in the troposphere is  $m^2 s^{-3}$

The turbulence dissipation rate ( $\epsilon$ ) in the troposphere is typically expressed in units of  $m^3/s^3$ . While the exact value varies depending on location, altitude, weather conditions, and the specific type of turbulence, a representative range is:

$\epsilon = 10 \text{ to } 100 \text{ } m^3/s^3$

Therefore, the statement is correct in terms of the units of turbulence dissipation rate, but incomplete without specifying a value within the typical range for the troposphere.

**Figure S4.** The query “the turbulence dissipation rate in the troposphere is  $m^2 s^{-3}$ ” was submitted. The initial output from software quantitatively characterized turbulence intensity in both the troposphere and the stratosphere.



Urbanization increases rainfall by %

Research suggests that urbanization can increase rainfall downwind by anywhere from 5% to 25% under certain conditions. However, the exact percentage varies depending on several factors, including:

- Size and type of urban area: Larger cities tend to have a greater impact.
- Geographic location: Coastal cities might experience different effects than inland cities.
- Climate: And regions might see more pronounced changes than humid regions.
- Meteorological conditions: The effect is strongest when there are pre-existing weather systems in place.
- How rainfall is calculated: Rainfall changes can be measured using different methods which yield varying results.

**Figure S5.** The query “Urbanization increases rainfall by %” was submitted. The output from software was demonstrably clearer than that of ChatGPT-4.



**Figure S6.** The query “Meteor radar data can be downloaded from” was submitted. The software provided numerous website suggestions. In contrast, ChatGPT-4 was unable to provide an accurate download website address.

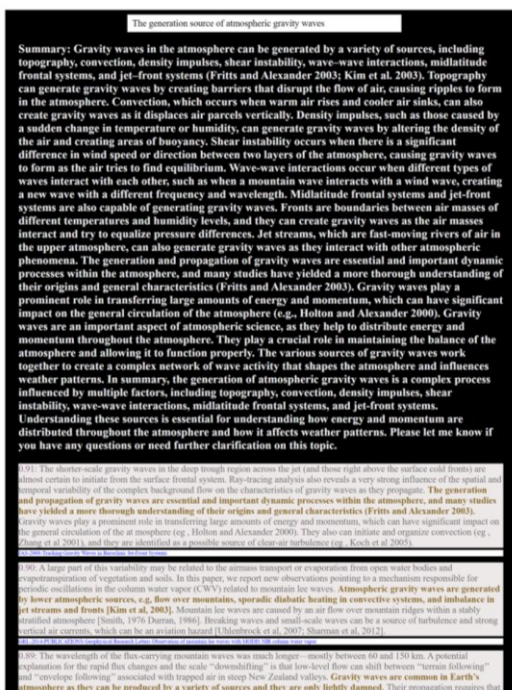


**Figure S7.** The query “The generation source of atmospheric gravity waves” was submitted. The bold, white text represents the summary generated by an LLM (Llama 2 70B). This summary correctly references the work of Fritts & Alexander (2003), a seminal publication in the field of gravity waves. In contrast, outputs from ChatGPT-4 failed to elucidate the full mechanism of gravity wave generation, including processes such as wind shear and wave-wave interactions.

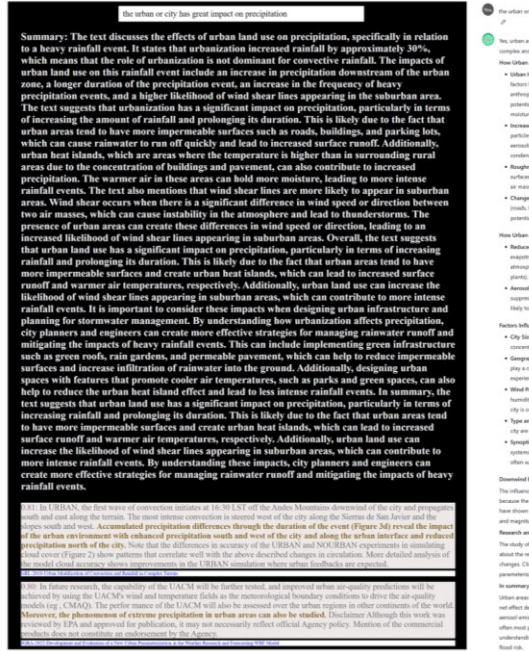
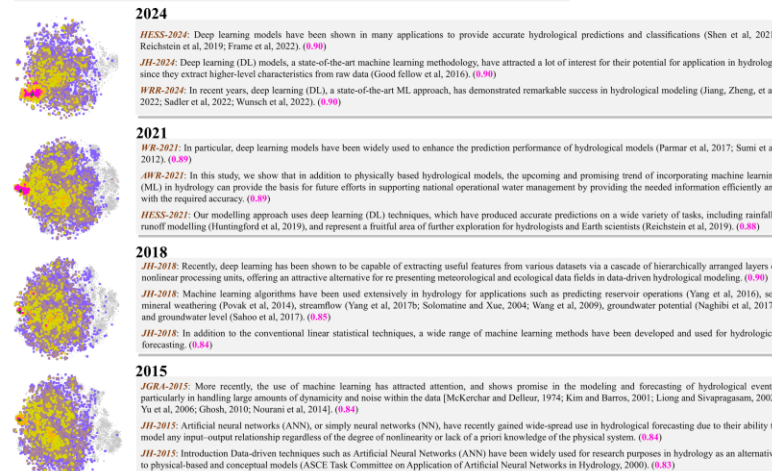


**Figure S8.** The query “the urban or city has great impact on precipitation” was submitted. The LLM summary (Llama 2 70B) can accurately capture the data presented in Fig. S5.

**Human query:** Machine learning and deep learning have advantages in hydrological modelling



**Human query:** Machine learning and deep learning have limitations in hydrological modelling.

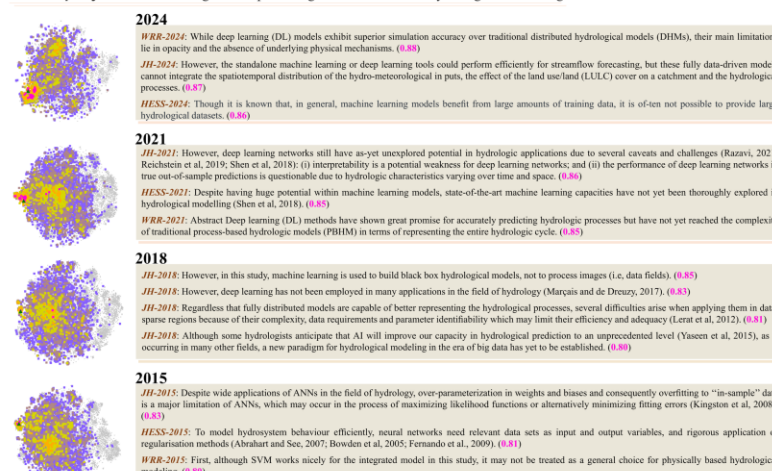


**Figure S9.** Taking “machine learning and deep learning in hydrological modelling” as an illustrative example to explore semantic search across two semantically similar tasks. The human queries are “Machine learning and deep learning have advantages in hydrological modelling” (above) and “Machine learning and deep learning have limitations in hydrological modelling” (down). Sentence libraries from the years 2024, 2021, 2018, and 2015, containing the keywords “hydro” (case-insensitive) and “model” (case-insensitive) are utilized. The total number of sentences ranges from 8,898 in 2015 to 22,155 in 2021. All sentences are transformed into 1024-dimensional dense vectors using PSTM\_4. The top-ranked sentences for each year are displayed in the colored box.

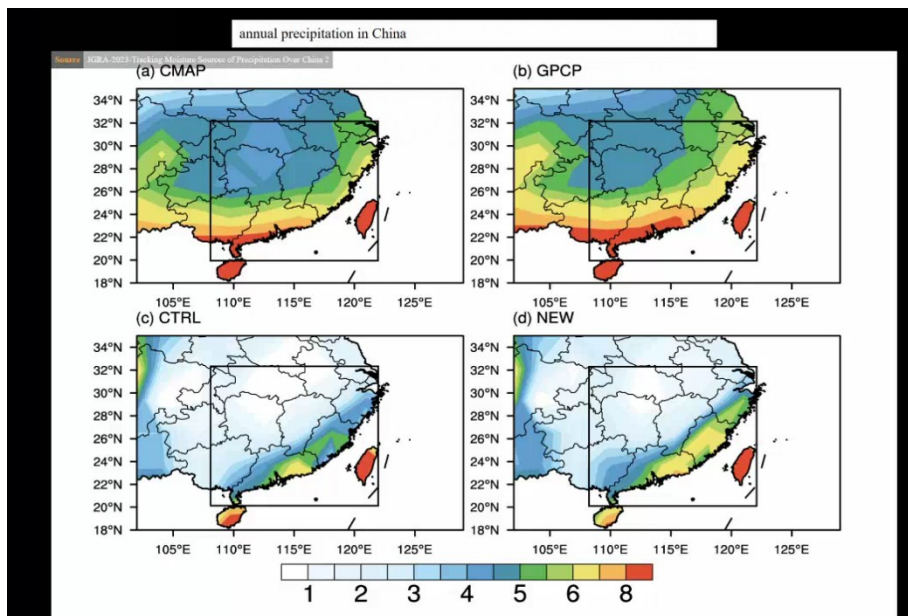


**Figure 1.** Mean August precipitation ( $\text{mm d}^{-1}$ ) in southern China during 1979–2008: observational data of (a) CPC Merged Analysis of Precipitation (CMAP) and (b) Global Precipitation Climatology Project (GPCP), and results of simulations (c) control experiment (CTRL) and (d) NEW. Rectangles represent the study area ( $20^{\circ}$ – $32^{\circ}$ N,  $108^{\circ}$ – $122^{\circ}$ E).

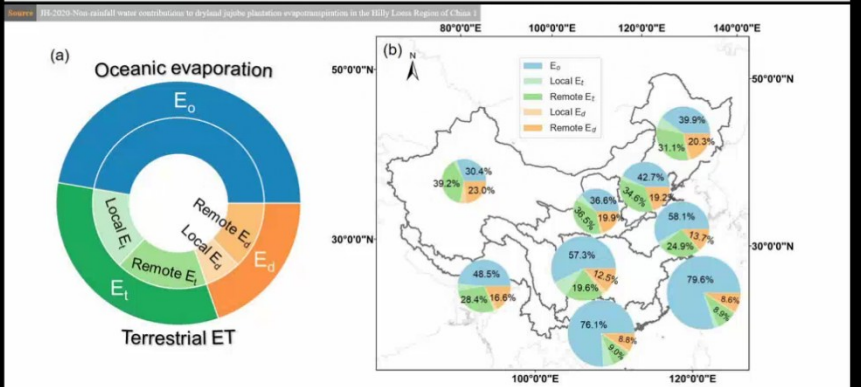


**Figure 2.** The multi-year average contribution rate from different moisture sources to precipitation over China (a) and over the nine river basins in China (b).

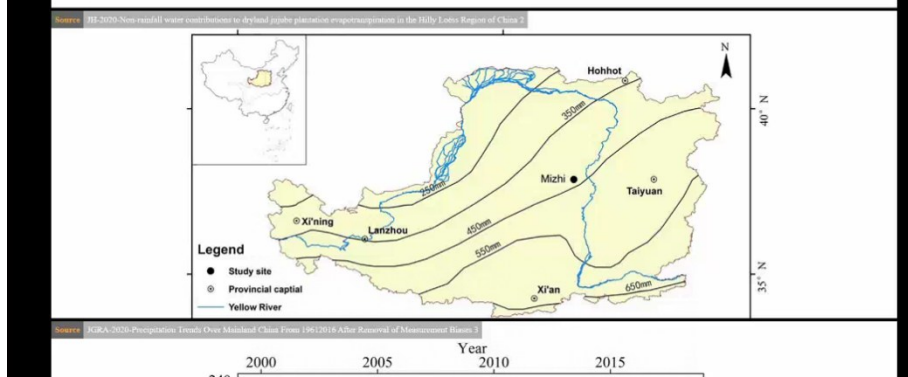


**Figure S10.** Professional image retrieval software can identify related images by performing semantic matching between user-provided prompts and academic paper image captions. This approach enables students, teachers or researchers to efficiently locate professional images with a high resolution. For instance, the prompt “annual precipitation in China” was submitted.

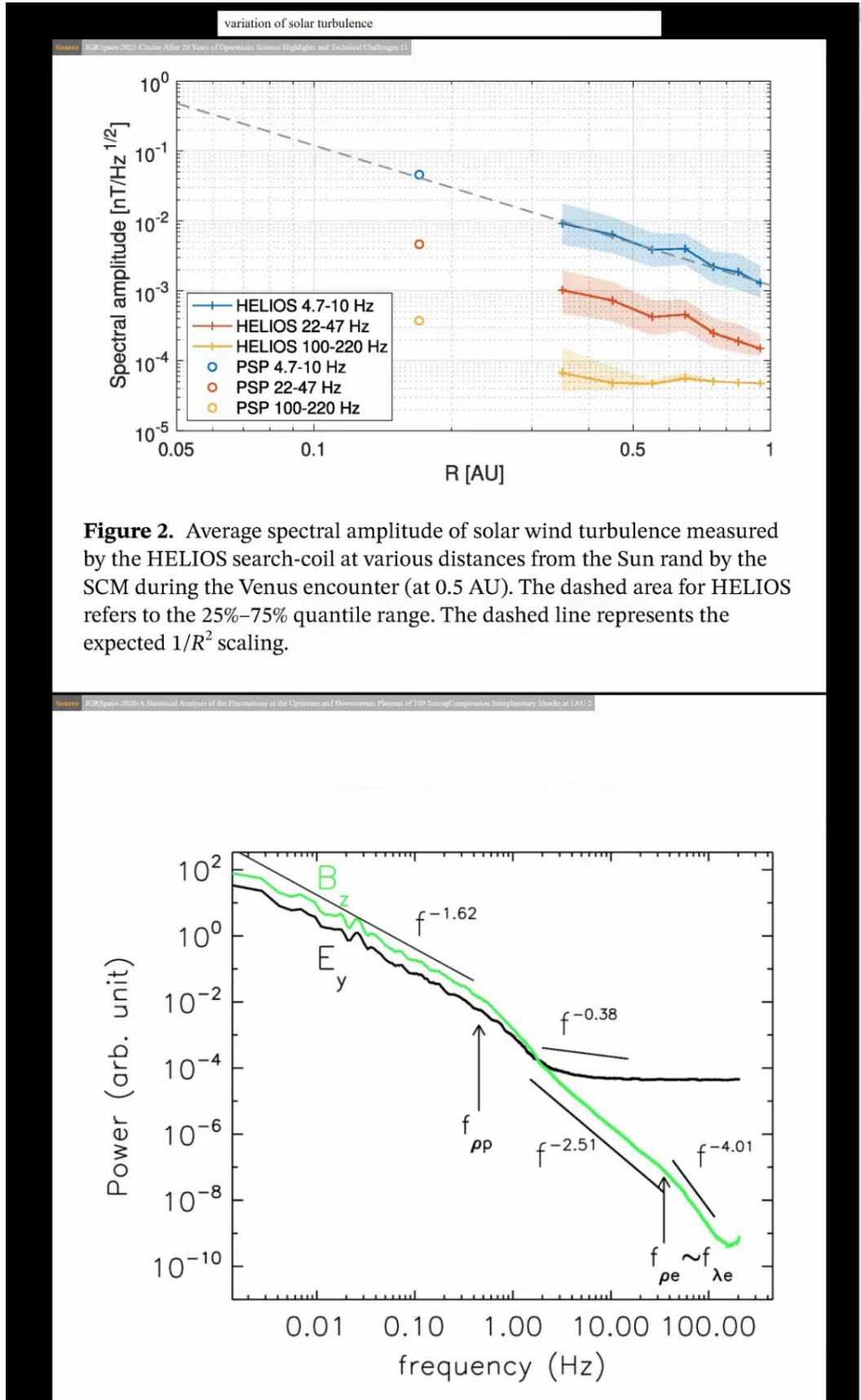


**Figure 2.** Average spectral amplitude of solar wind turbulence measured by the HELIOS search-coil at various distances from the Sun and by the SCM during the Venus encounter (at 0.5 AU). The dashed area for HELIOS refers to the 25%–75% quantile range. The dashed line represents the  $1/R^2$  scaling.